Studies on development of analytical methods to quantify protein aggregates and prediction of soluble/insoluble aggregate-formation

Jun Fukuda

2015

Contents

1 General Information

Study of proteins, especially monoclonal antibodies as therapeutics has recently attracted a great deal of attention from the pharmaceutical industry. In the last 20 years, over twenty monoclonal antibodies have been approved in various therapeutic categories [1]. As shown in Table 1, twenty biologics pharmaceuticals and six antibody pharmaceuticals including Humira® (adalimumab) and Remicade® (infliximab) which are ranked as the two highest ranks have already been ranked in the sales top 30 of pharmaceuticals in 2012 [2]. These biopharmaceutical products have been drastically improving the quality of life of patients.

Compared to small pharmaceutical molecules, therapeutic protein products are considerably large entities with inherent physicochemical complexity. Therefore, many physical and chemical factors may lead to protein degradation and consequently affect the quality of therapeutic protein products during manufacturing, storage, shipping and handling steps [3-5]. Chemical degradation of proteins involves fragmentation, oxidation (mostly occurring at methionine and tryptophan residues), deamidation (mostly occurring at asparagine residues) and disulfide scrambling. Physical degradation of proteins involves unfolding, dissociation, denaturation, adsorption, precipitation processes and aggregates [5]. Their efficacy and safety should be evaluated and they should be controlled on the basis of their risk.

Immune response or immunogenicity of the therapeutic proteins remains one of the major risks. The testing of the immune response to these biological products such as the anti-drug antibodies (ADA) are an important part of the product development and post marketing monitoring of drug safety [6]. The appearance of antibodies against the drug can trigger safety issues such as autoimmune disorders by neutralizing the endogenously secreted proteins. The major causes of immunogenicity to the pharmaceutical proteins are still unclear, but protein aggregates are suspected to trigger an immune response [7, 8]. For example, it is reported that the presence of aggregates in human growth hormone (hGH) products correlated with an increased frequency of immune response in the patients [9]. A storage temperature of interferon-alpha (IFN-alpha) vial also correlated with the increase in the immunogenicity. The immunogenicity increased when the vials

were stored at ambient temperature which could cause increases in aggregates, but not when stored at 4°C [9]. Furthermore, since it was shown that IFN-alpha aggregates could induce auto antibody in human IFN-alpha transgenic mice, the key factor of the immune response to IFN-alpha is expected to be the aggregate species [10]. The enhancement of immunogenicity of protein aggregates is interpreted by their multiple-epitope character and/or conformational changes of the aggregated protein molecules [11].

Therefore, protein aggregates are considered a critical attribute in terms of their potential to elicit immune response and affect the product activity, enhancing or diminishing potency. For this reason, aggregates in protein pharmaceuticals should be accurately quantified, characterized in detail and minimized as possible.

In this study for accurately quantification of protein aggregates, we propose a new size exclusion chromatography (SE-HPLC) method that can separate the polysorbates that interfere with aggregate quantitation in SE-HPLC from protein samples in an on-line mode using a precolumn with mixed characteristics of size exclusion phase and reversed-phase (chapter 1). Then, we examined the effect of the setting parameters on fractographic characteristics and attempted to adjust the conditions of the Hollow fiber flow field flow fractionation (HF5, Figure 1 shows schematic diagram of the principle of HF5) that can be orthogonal method to SE-HPLC such as analytical ultracentrifugation-sedimentation velocity (AUC) and asymmetric flow field flow fractionation (AF4) for quantification of monoclonal antibody aggregates (chapter 2).

In this study for characterization and minimization of protein aggregates, we used eight kinds of immunoglobulin G (IgG) 1 as model protein pharmaceuticals, and five physicochemical parameters experimentally evaluated and two physicochemical parameters calculated based on the information from the amino acid sequence, as explanatory valuables to be related to the aggregate formation. The aggregation formation data were correlated to the experimental and the calculated parameters. Multivariate analysis was done based on Akaike's Information Criterion (AIC) [12, 13] to pick out the important explanatory parameters to characterize the aggregate formation. We also discuss the mechanism and the potent approach to suppress the soluble and insoluble aggregate formation of IgG.

Table 1 Top 30 of global sales of therapeutic drugs in 2012

	Trade name	Generic name	Type	Category/Effect	Sales (million$)
1	Humira®	Adalimumab	Biologic	Rheumatoid arthritis	9,603
2	Remicade®	Infliximab	Biologic	Rheumatism	9,071
3	Embrel®	Etanercept	Biologic	Rheumatoid arthritis	8,476
4	Adoair®	Salmeterol	Small molecule	Antiasthmatic agent	8,216
5	Crestor®	Rosuvastatin	Small molecule	Hypolipidemic agent	7,430
6	Rituxan®	Rituximab	Biologic	Non-Hodgkin's lymphoma	7,227
7	Lantus®	Insulin Glargine	Biologic	Diabetes	6,555
8	Herceptin®	Trastuzumab	Biologic	Breast cancer	6,444
9	Avastin®	Bevacizumab	Biologic	Metastatic colon cancer	6,307
10	Januvia®	Sitagliptin	Small molecule	Type II diabetes	6,208
11	Diovan®	Valsartan	Small molecule	Antihypertensive agent	5,793
12	Plavix®	Clopidogrel	Small molecule	Antiplatelet agent	5,277
13	Cymbalta®	Duloxetine	Small molecule	Serotonin noradrenaline reuptake inhibitor	5,107
14	Abilify®	Aripiprazole	Small molecule	Schizophrenia	5,105
15	Lipitor®	Atorvastatin	Small molecule	Hyperlipidemia	5,028
16	Spiriva®	Tiotropium	Small molecule	Chronic obstructive pulmonary disease	4,707
17	Glivec®	Imatinib	Small molecule	Anticancer agent	4,675
18	NovoRapid®	Insulin aspart	Biologic	Diabetes	4,436
19	Lyrica®	Pregabalin	Small molecule	Nerve pain	4,320
20	Singulair®	Montelukast	Small molecule	Antiasthmatic agent	4,314
21	Nexium®	Esomeprazole	Small molecule	Antiulcer agent	4,195
22	Prevenar®	Pediatric pneumococcal vaccine	Biologic	Infection prophylaxis	4,117
23	Neulasta®	Pegfilgrastim	Biologic	Neutropenia	4,092
24	Lucentis®	Ranibizumab	Biologic	Macular degeneration	4,019
25	Copaxone®	Glatiramer	Small molecule	Multiple sclerosis	3,968
26	Revlimid®	Lenalidomide	Small molecule	Multiple Myeloma	3,767
27	Atripla®	Efavirenz	Small molecule	Anti-HIV agent	3,574
28	Symbicort®	Budesonide	Small molecule	Antiasthmatic agent	3,516
29	Epogen®	Epoetin alfa	Biologic	Renal anemia	3,448
30	Micardis®	Telmisartan	Small molecule	Antihypertensive agent	3,386

Source: Homepage of Cogedim Strategic Data K. K. (partially, modified) [2]

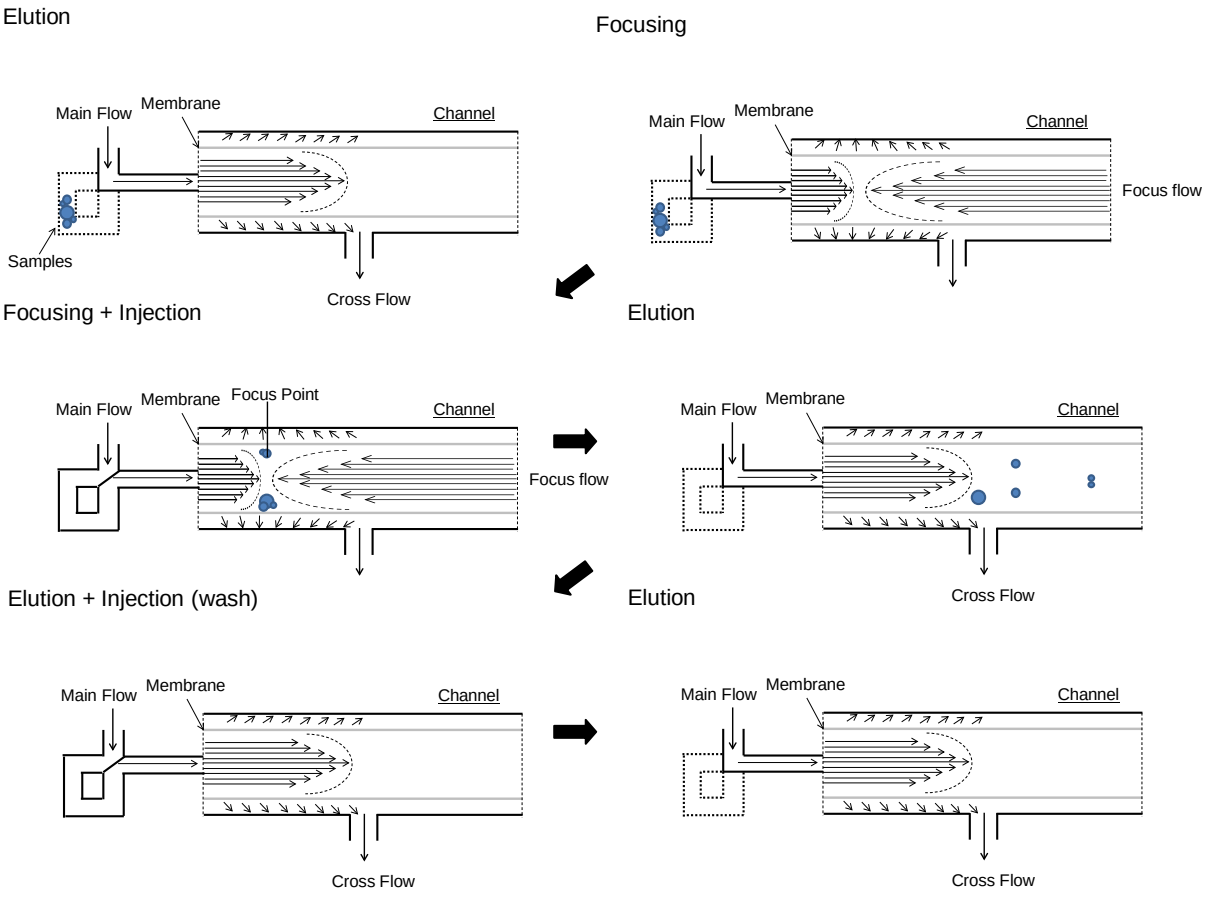

Fig. 1. Schematic diagram of the principle of HF5

1.1 Reference

[1] Reichert JM (2008) Curr Pharm Biotechnol 9:423-430

[2] http://www.utobrain.co.jp/news/20130724.shtml

[3] Cromwell ME, Hilario E, Jacobson F (2006) AAPS J 8:E572–E579

[4] Wang W (1999) Int J Pharm 185:129–188

[5] Filipe V, Hawe A, Carpenter JF, Jiskoot W (2013) Tr Anal Chem 49:118–125

[6] Wadhwa M, Bird C, Dilger P, Gaines-Das R, Thorpe R (2003) J. Immunol. Methods 278:1–17

[7] Rosenberg A.S (2006) AAPS J. 8: E501-E507

[8] Schellekens H (2008) Biotechnol. Annu. Rev. 14: 191-202

[9] Moore WV, Leppert P (1980) J. Clin. Endocrinol. Metab. 51: 691-697

[10] Braun A, Kwee L, Labow MA, Alsenz J (1997) Pharm. Res. 14: 1472-1478

[11] Hermeling S, Crommelin DJ, Schellekens H, Jiskoot W (2004) Pharm. Res. 21: 897-903

[12] Akaike H (1974) IEEE Transactions on Automatic Control 19: 716–723.

[13] Hurvich CM, Tsai CL (1989) Biometrika 76; 297-307

2 Utilization of a precolumn with size exclusion and reversed-phase modes for size-exclusion chromatographic analysis of polysorbate-containing protein aggregates (Chapter 1)

2.1 Introduction

Nowadays, protein-based pharmaceutical products have rapidly been advanced. The situation increases demands for development of analytical technologies for protein aggregates, which are common sources of protein instability and are considered to concern their potential to elicit immune responses [1-5]. Various analytical methods that can evaluate protein aggregates have been developed such as analytical ultracentrifugation and asymmetric field flow fractionation [6-10]. However, these methods still have several weak points, for example, low throughput, need for professional skills, or difficulty in method development [10]. In contrast, size-exclusion high performance liquid chromatography (SE-HPLC) with high throughput capacity and highly quantitative performance is frequently used and indispensable for quantification of protein aggregates.

In SE-HPLC, proteins and their aggregates are separated based on the difference in the permeation property into pores of stationary phase (e.g., silica-based polymeric beads). Larger molecules (e.g., aggregates) or non-spherical (e.g., straight chain) molecules in a mixture are rapidly excluded and therefore eluted from the resin pores, while smaller molecules with greater access to the pores are eluted more slowly [11]. In many marketed biopharmaceuticals, nonionic surfactants such as polysorbate 80 (PS80) and polysorbate 20 (PS20) are included as stabilizers to protect the active protein against denaturation or aggregate formation [12–16]. The molecular mass of the polysorbates is usually lower than that of most of proteins and protein aggregates. However, the polysorbates present in some formulations are eluted at retention times close to those of protein aggregates and then interfere with aggregate quantitation in SE-HPLC. This interference becomes a serious problem to perform sensitive and quantitative SE-HPLC methods capable of quantitating protein aggregates in formulated products. Unfortunately, it is very difficult to selectively separate detergents from protein solutions. Some methods are reported to separate detergents from protein solutions [17-22], but these methods take time because they cannot be connected directly to an

analytical column and the recovery of protein is not 100%. Gunturi et al. proposed to utilize potassium phosphate buffer containing isopropyl alcohol as a mobile phase in SE-HPLC [23]. They found that the peaks of the polysorbates were completely disappeared when isopropyl alcohol content was increased up to 20–25% range in the mobile phase [23]. However, isopropyl alcohol at such high concentrations may cause some damage to proteins. Therefore, some separation methods without use of organic solvents are strongly desired for long time. In this study, we will propose a new SEC-HPLC method that can separate the polysorbates from protein samples in an on-line mode using a precolumn with mixed characteristics of size exclusion phase and reversed-phase. We will also show the significance of the temperature control in the on-line separation to perform sensitive and quantitative SE-HPLC methods.

2.2 Experimental

2.2.1 Chemicals and reagents

Sodium monobasic phosphate, sodium dibasic phosphate and human serum albumin (HSA, lyophilized powder, Fatty acid free, globulin free, ≥ 99%, product # A3782) were from Sigma-Aldrich (St. Louis, MO, USA). Sodium chloride (NaCl) was from Wako Pure Chemicals (Tokyo, Japan). Dulbecco's phosphate-buffered saline (PBS) was from Nissui Seiyaku (Tokyo, Japan). Polysorbate 80 (PS80) was from NOF Corp. (Tokyo, Japan), while polysorbate 20 (PS20) was from Croda (East Yorkshire, England). Synagis injection containing Palivizumab was purchased from Abbvie (IL, USA). The pure standard sample of recombinant human erythropoietin (r-HuEPO) was obtained from Kyowa Hakko Kirin (Tokyo, Japan).

2.2.2 Sample preparations

HSA and synagis injection were reconstituted by addition given amount of water and dialyzed with PBS for 24 h. The HSA was diluted with the PBS to 3 mg/mL, and the synagis injection was diluted with the PBS to 1 mg/mL. The commercially available r-HuEPO was also dialyzed with the PBS and diluted with the PBS to 1 mg/mL. Heat-induced r-HuEPO aggregate-containing samples were prepared by heating the diluted r-HuEPO sample for one day at 40 °C. PS80 and PS20 were

diluted with the PBS to 0.01, 0.02, 0.05, 0.1, 0.2, 0.5 and 1 mg/mL. All the samples were stored at 2-8 °C until the HPLC characterization described in Section 2.2.3.

2.2.3 SE-HPLC methods

SE-HPLC was performed with an Agilent 1100 chromatography system connected to a Tosoh TSKgel G3000SW$_{XL}$ (300 × 7.8 mm, 5 μm particle size). The chromatographic control, data acquisition and data analysis were performed using Chemstation (Agilent Technologies). The samples were set on an auto-sampler (as an accessory of the Agilent 1200 chromatography system) at 4 °C in a refrigerator. The UV detector was operated at a wavelength of 215 nm. The mobile phases for the SE-HPLC method were the PBS (HSA, r-HuEPO) and 50 mM NaH_2PO_4/Na_2HPO_4 500 mM NaCl pH7 (synagis injection). The mobile phase was filtered with a 0.45-μm Millipore filter and was degassed with an online degasser. The flow rate was 0.5 mL/min and the column was maintained at 25 °C unless otherwise noted. In order to prevent automatic stopping (due to condensation detection at lower temperatures), the leak sensor of the column oven was turned off. The method run time was set to 40 min.

A Shodex MSpak GF-4A (10 × 4.6 mm, 9 μm particle size) was used as a precolumn to separate the polysorbates. The column, when necessary, was connected to the front of the main column (Tosoh TSKgel G3000SW$_{XL}$) with a stainless steel capillary and fittings.

2.3 Results and discussion

2.3.1 SE-HPLC characteristics of HSA aggregates and polysorbates

Figure 1 shows chromatograms of the HSA sample and the diluted polysorbate samples on the SEC-HPLC system without the precolumn at 215 nm. Spectrophotometric detection of proteins is frequently performed at 280 nm based on the absorption of tryptophan and aromatic amino acid residues. However, the photometric detection at 215 nm due to amide bonds is required for highly sensitive detection of protein targets at extremely low concentrations such as protein aggregates in protein-based pharmaceutical products. The main peak at a retention time of 17 min corresponds to HSA monomer, while the peaks at 15, 14.5, 14 min correspond to dimer, trimer and tetramer of

HSA, respectively. Larger aggregates were eluted in the region of retention times from 11 to 14 min. In order to characterize the aggregation, the peak analysis of this region is very important. Unfortunately, PS80 and PS20 were eluted at retention times very close to that of as the aggregates of HSA. Although the molecular mass of PS80 and PS20 are smaller than that of HSA, the polysorbates were eluted at retention times earlier than the time expected from the molecular mass. The reason may be that PS80 and PS20 can be formed in a micellar state in an aqueous solvent. This is a typical example of the interference from PS80 and PS20 in the SE-HPLC quantification of aggregate contents as reported before [23].

We tried in this work to separate the polysorbate's peaks from the protein-derived ones by using a precolumn method because on-line analysis without any specific separation pretreatment of protein samples is convenient for chromatographic analysis of protein aggregates in protein-based pharmaceutical products. One of separation modes to be utilized for this purpose may be electrostatic interaction in anion or cation exchange. However, separation conditions for ion exchange chromatography have to be tuned for every protein, because the isoelectric points of proteins are different from each other. Another separation mode may be hydrophobic interaction in reversed-phase. One of weak points of this method is that the method requires organic solvents or ammonium sulfate in elution buffer. The situation may give some damages to proteins and may cause the dissociation of some non-covalent aggregates in reversed-phase chromatography and hydrophobic interaction chromatography. As a result, we have considered that some porosity silica gel with some hydrophobic characteristics may be effective to remove hydrophobic surfactants with relatively large molecular mass such as PS80 and PS20. In preliminary experiments we tried to use two kinds of anion exchange columns, one anion/cation multi-mode column and several reversed-phase columns as precolumn. However, these columns were not efficient for this purpose. We finally focused on Shodex MSpak GF-4A, which has been developed for column-switching method to eliminate surfactant from surfactant-containing protein/peptide samples. Although MSpak GF-4A is mainly used for LC-MS because surfactants degrade LC-MS columns and decrease the reproducibility of LC-MS, we tried to use MSpak GF-4A as a precolumn connected to SEC column and to develop a new online SE-HPLC method without column-switching system.

As expected, on the SE-HPLC system without MSpak GF-4A, the peak area of PS80 and PS20 increased in proportion to the injection amount of the polysorbates (Fig. 2A, B; black triangle). In contrast, when MSpak GF-4A was connected as a precolumn to the SE-HPLC system, the PS80 peak was not detected at least up to 8-μg injection (Fig. 2A; gray triangle). Very small peak of PS80 was detected at 20-μg injection and clearly detected at 40-μg injection with an area of 170 mAU×sec. However, the peak area was much smaller than those observed in the separation without MSpak GF-4A. In the case of PS20, only very small peak was detected even at 20-μg and 40-μg injections when the MSpak GF-4A column was used (Fig. 2B; gray triangle). These results indicate that the MSpak GF-4A precolumn is very effective to trap PS80 and PS20 in the on-line mode. The limiting value of the trapping is about 10 μg for PS80 and 20 μg for PS20. The difference of the trapping characteristics between PS20 and PS80 seem to be ascribed to multiplier effect of mixed characteristics of size exclusion phase and reversed-phase of the precolumn. Actually the difference cannot be simply explained from the hydrophobic properties of the polysorbates, and precolumns with the revered-phase characteristics alone did not work well to trap the polysorbates selectively. When 40 μg of PS80 was injected to the precolumn-SE-HPLC system, the precolumn must be saturated with PS80. Therefore the succeeding injection of even small amounts of PS80 (for example 8 μg) could not be trapped. However, the PS80-suturated precolumn can still trap PS20. PS20 was scarcely detected at 20-μg injection when the PS80-saturated precolumn was use. It is noteworthy that the detergent trapped in MSpak GF-4A is easily washed out with mixed aqueous mobile phase containing organic solvents such as acetonitrile. Actually, the precolumn was cleaned with acetonitrile (30% v/v)-containing aqueous mobile phase after each analysis unless otherwise noted, when large amounts of polysorbates were injected.

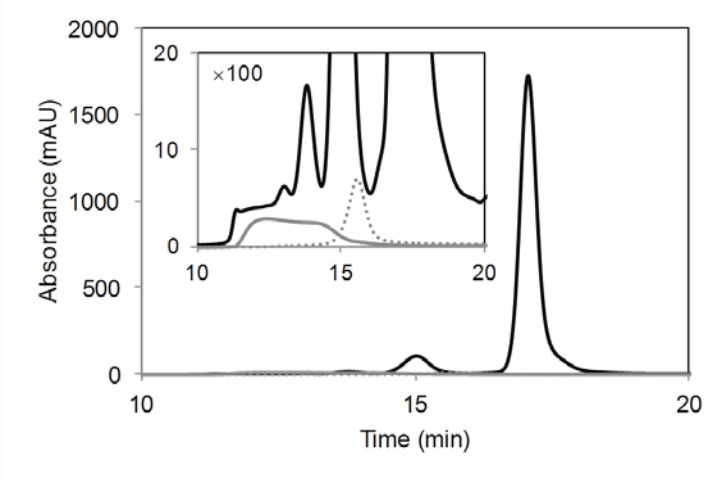

Fig. 1. Chromatograms of the HSA sample (black solid line; 3 mg/mL × 10 μL), diluted PS80 sample (gray solid line; 1 mg/mL × 40 μL) and the diluted PS20 sample (gray dash line; 1 mg/mL × 40 μL) on the SEC-HPLC system without the precolumn at 25 °C (flow rate: 0.5 mL/min, UV detection: 215 nm).

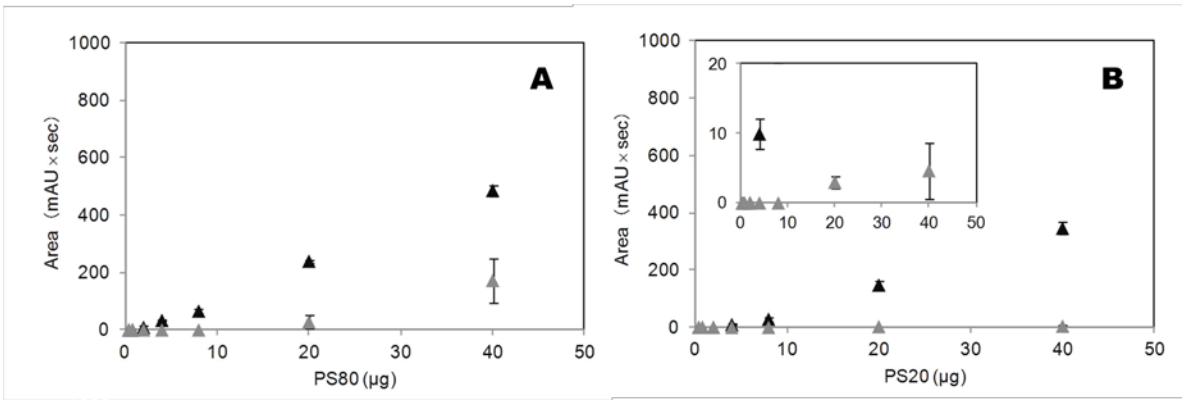

Fig. 2. Effects of the precolumn MSpak GF-4A on the peak area of (A) PS80 and (B) PS20 detected on the SEC-HPLC system; (black triangle) without or (gray triangle) with the precolumn MSpak GF-4A. The error bars indicate the standard deviation (*n* = 3).

2.3.2 Effects of temperature on the one separation of protein aggregates on SE-HPLC with MSpak GF-4A

As described in Section 2.3.1, the MSpak GF-4A is very effective to trap polysorbates. However, it was found that the chromatograms of the HSA sample depend on the column temperature (Fig. 3A). Figure 4A shows the dependence of the total peak area of the HSA aggregates on the column temperature. The peak area of the HSA aggregate increased with an increase in the column temperature from 5 °C to 20 °C and reached a constant value above 20 °C at least up to 30 °C (Fig. 4A, gray square), although the HSA monomer peak area was not affected by the column temperature (data not shown). In contrast, when only the SE column was used without the precolumn, the total peak area of the aggregate and monomer was independent of the column temperature (data not shown). These results suggest that the HSA aggregates are specifically trapped on the MSpak GF-4A precolumn at lower temperatures predominantly by hydrophobic interaction. It has been reported that the high-order structure of protein aggregates usually differs from that of the monomer [24-26], although some protein aggregates seem to retain the high-order structure similar to that of monomer [26, 27]. In the case of HSA, the fluorescence spectral characteristics of the aggregates are different from those of the monomer (data not shown). This evidence suggests the change in the high-order structure on the aggregation. Since the aggregates are susceptible to the adsorption on the precolumn at lower temperatures, the hydrophobic interaction between the aggregates and the stationary phase of the precolumn seems to be a major contribution to trap the aggregates on the precolumn. The hydrophobic interaction decreases with an increase in the column temperature, and the HSA aggregates can pass through the precolumn at column temperatures over 20 °C.

In contrast, the peak area of the heat-induced r-HuEPO aggregates decreased with an increase in the column temperature (Fig. 3B and Fig. 4B (gray diamond)) on the SE-HPLC system with MSpak GF-4A. The limiting value of the peak was observed at column temperature lower than 10 °C. The peak area of the r-HuEPO monomer was independent of the column temperature at least in the range from 5 to 30 °C as in the case of the HSA monomer. These phenomena may be caused by

the high-order conformational change of the heat-induced r-HuEPO aggregates at increased column temperatures to induce the exposure of these hydrophobic surface.

We also show another example of the column temperature dependence of protein aggregates.

As shown in Figs. 3C and 4C, the peak shape and the area of the aggregate (dimer, peak 1) and monomer in the synagis injection are independent of the column temperature in the range from 5 °C to 30 °C. The synagis injection dimer seems to have characteristics similar to those of the monomer in view of the high-order structure and the surface property. The hydrophobic interaction between the synagis injection aggregate and the stationary phase of the MSpak GF-4A column is not so strong, as in the case of the monomer of the other proteins examined here.

Anyway, it is very important to control the column temperature to avoid the adsorption of protein aggregetes in the MSpak GF-4A precolumn. The optimum temperature of the column must be selected for individual protein targets.

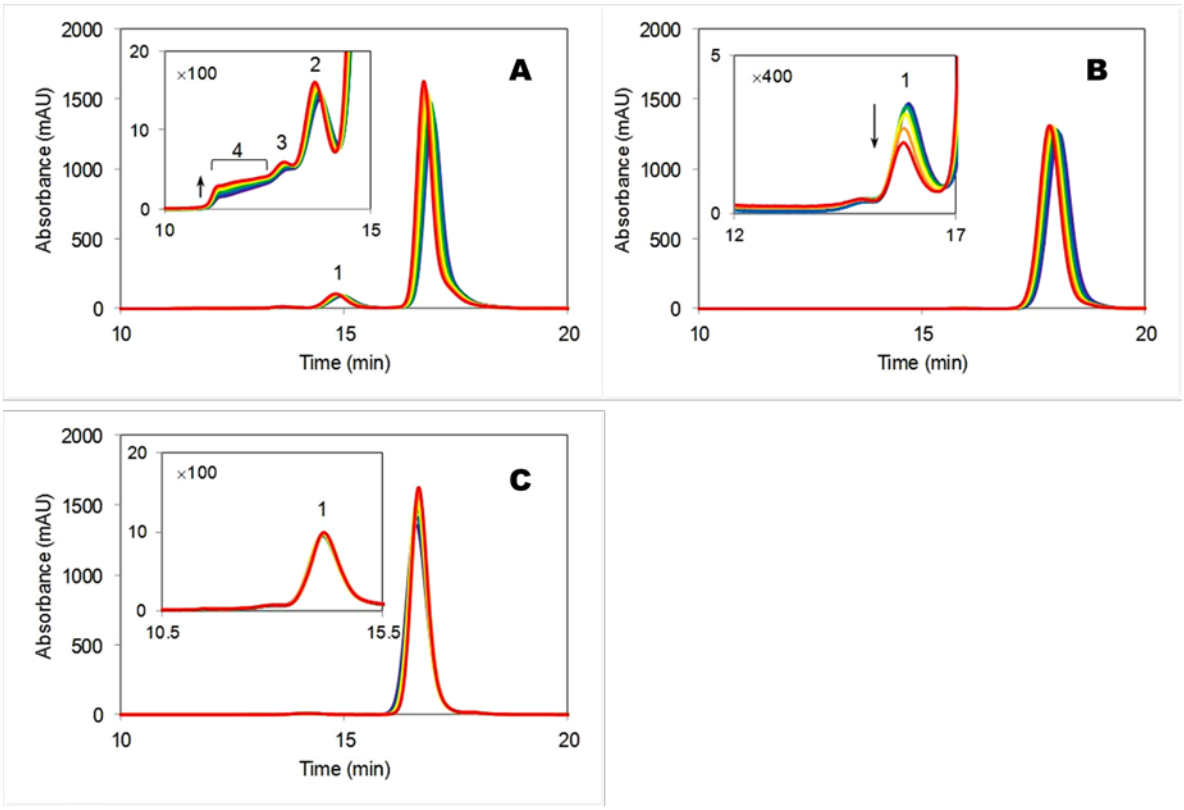

Fig. 3. Chromatograms of (A) the HSA sample (3 mg/mL × 10 μL), (B) heat-induced r-HuEPO sample (1 mg/mL × 30 μL), (C) synagis injection sample (1 mg/mL × 20 μL) on the SE-HPLC system with MSpak GF-4A at various column temperatures. Purple, blue, green, yellow, orange and red lines are each protein samples analyzed at 5, 10, 15, 20, 25 and 30°C respectively. The peaks numbered as 1, 2, 3 and 4 of the HSA aggregates correspond to the dimer, trimer, tetramer and larger oligomer(s), respectively. Peak 1 of heat-induced r-HuEPO and synagis injection corresponds to the dimer.

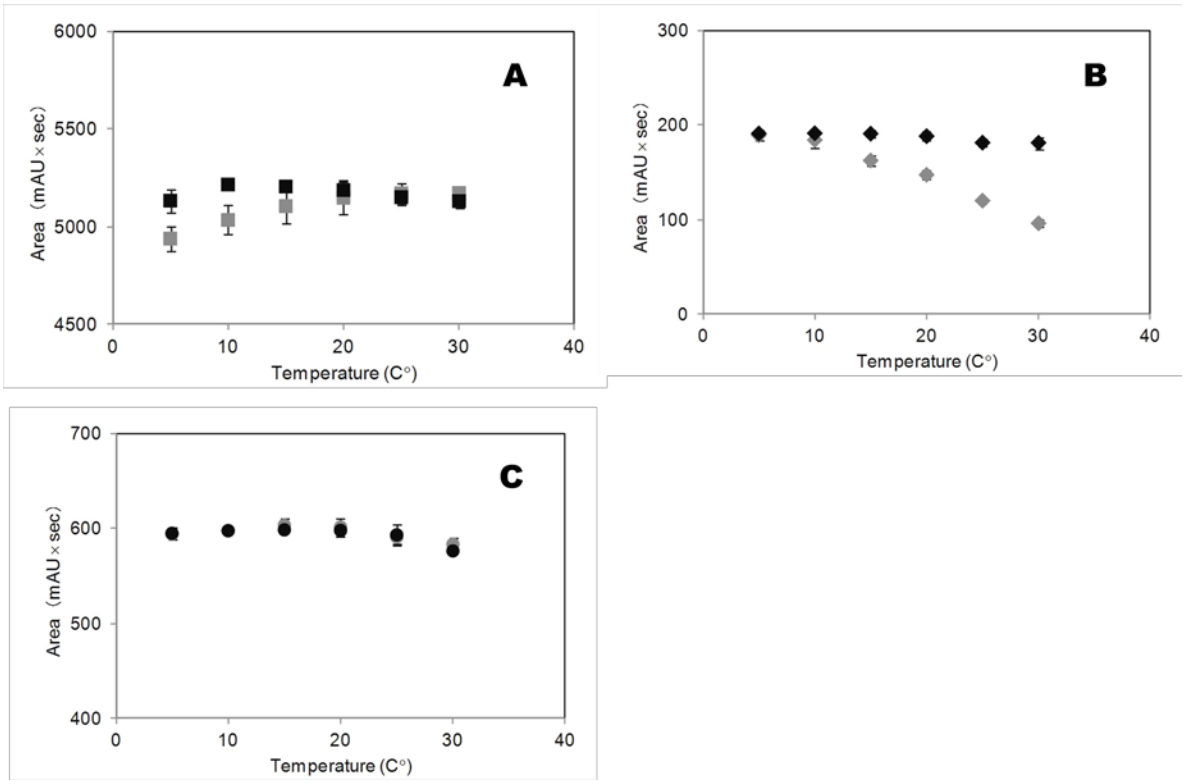

Fig. 4. Effects of the column temperature on the total peak areas of the aggregates in (A) the HSA sample on the SE-HPLC system with MSpak GF-4A (gray squares) and without MSpak GF-4A (black squares), (B) heat-induced r-HuEPO sample with MSpak GF-4A (gray diamonds) and without MSpak GF-4A (black diamonds) and (C) synagis injection sample with MSpak GF-4A (gray circles) and without MSpak GF-4A (black circles). The error bars indicate the standard deviation (n = 3).

2.3.3 HSA with and without PS80 analyzed by SE-HPLC with and without MSpak GF-4A

In the region from 10 to 15 min, the peak shape of HSA with PS80 was significantly different from that of HSA without PS80 by analyzing SE-HPLC without MSpak GF-4A (Fig 5-A). Not only aggregates but PS80 were eluted in the region. While, the peak shape of the HSA sample with PS80 on SEC-HPLC with MSpak GF-4A was almost the same as that of the HSA sample without PS80 on SEC-HPLC without MSpak GF-4A (Fig 5-B). PS80 was successfully trapped by MSpak GF-4A. The results clearly show that the connection of MSpak GF-4A to SEC column and the setting of proper column temperature (e.g., 25 °C for HSA) allow to perform quantification of protein aggregate contents, because MSpak GF-4A can effectively eliminate of the interference from PS80.

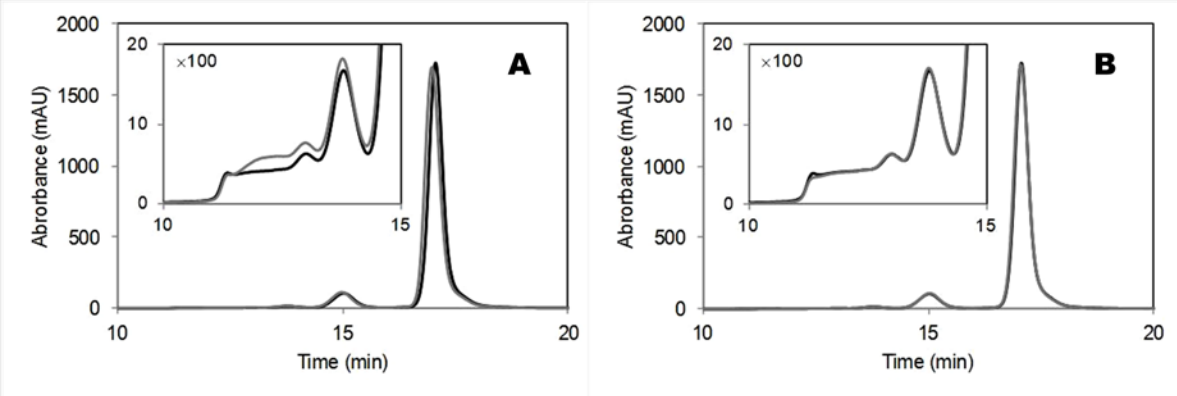

Fig. 5. (A) Chromatograms of HSA by SE-HPLC without MSpak GF-4A; black line corresponds to the HSA sample (3 mg/mL × 10 μL) without PS80 and gray line is the HSA sample containing PS80 (HSA: 3 mg/mL × 10 μL, PS80: 1 mg/mL × 10 μL). (B) Chromatograms of HSA; black line corresponds to the HSA sample (3 mg/mL × 10 μL) without PS80 on SEC-HPLC without MSpak GF-4A and gray line corresponds to the HSA sample containing PS80 (HSA: 3 mg/mL × 10 μL, PS80: 1 mg/mL 10 μL) by SE-HPLC with MSpak GF-4A.

2.4 Reference

[1] A. Eon-Duval, H. Broly, R. Gleixner, Biotechnol. Prog. 28 (2012) 608.

[2] A. S. Rosenberg, A. Worobec, BioPharm Int. 17 (2004) 22.

[3] A. S. Rosenberg, AAPS J. 8 (2006) 501.

[4] J. F. Carpenter, T. W. Randolph, W. Jiskoot, D. J. A. Crommelin, C. R. Middaugh, G. Winter, Y. X. Fan, S. Kirshner, D. Verthelyi, S. Kozlowski, K. A. Clouse, P. G. Swann, A. Rosenberg, B. Cherney, J. Pharm. Sci. 98 (2009) 1202.

[5] S. K. Singh, N. Afonina, M. Awwad, K. Bechtold-Peters, J. T. Blue, D. Chou, M. Cromwell, H. J. Krause, H. C. Mahler, B. K. Meyer, L. Narhi, D. P. Nesta, T. Spitznagel, J. Pharm. Sci. 99 (2010) 3302.

[6] P. Schuck, Biophys. J. 78 (2000) 1606.

[7] J. Lebowitz, M. S. Lewis, P. Schuck, Protein Sci. 11 (2002) 2067.

[8] J. Liu, J. D. Andya, S. J. Shire, AAPS J. 8 (2006) E580.

[9] T. Arakawa, J. S. Philo, D. Ejima, K. Tsumoto, F. Arisaka, BioProcess Int. 5 (2007) 36.

[10] T. Arakawa, J. S. Philo, D. Ejima, H. Sato, K. Tsumoto, BioProcess Int. 4 (2007) 52.

[11] M. Potschka, J. Chromatogr A 648 (1993) 41.

[12] Y. Endo, H. Nagai,Y.Watanabe, K. Ochi, T. Takagi, J. Biochem. 112 (1992) 700.

[13] L. Bam, J.L. Cleland, T.W. Randolph, Biotechnol. Prog. 12 (1996) 801.

[14] M. Katakam, L.N. Ell, A.K. Banga, J. Pharm. Sci. 84 (1995) 713.

[15] B. S. Chang, B. S. Kendrick, J. F. Carpenter, J. Pharm. Sci. 88 (1996) 1345.

[16] B. A. Kerwin. J. Pharm. Sci. 97 (2008) 2924.

[17] P. Neves, S. C. D. N. Lopes, I. Sousa, S. Garcia, P. Eaton, P. Gameiro, J. Pharm. Biomed. Anal. 49 (2009) 276.

[18] M. Linetsky, K. Johar, J. Meltretter, S. Padmanabha, T. Parmar, A. R. Vasavada, M. Pischetsrieder, R. H. Nagaraj, Arch. Biochem. Biophys. 514 (2011) 16.

[19] M. J. Troese, A. Kahlon, S. A. Ragland, A. K. Ottens, N.Ojogun, K. T. Nelson, N. J. Walker, D. L. Borjesson, J. A. Carlyon, Infect. Immun. 79 (2011) 4696.

[20] K. M. Clarka, N. Fedoriwa, K. Robinsona, S. M. Connellyb, J. Randlesa, M. G. Malkowskic, G. T. DeTittac, M. E. Dumont, Protein Expr. Purif. 71 (2010) 207.

[21] L. Guerrier, I. Flayeux, E. Boschetti, M. B. Radosevich, J. Chromatogr. B, 664 (1995) 119.

[22] R. C. Bruch, N. R. Thotakura, O. P. Bahl, J. Biol. Chem. 261 (1986) 9450.

[23] S. R. Gunturi, I. Ghobrial, B. Sharma, J. Pharm. Biomed. Anal. 43 (2007) 213.

[24] R. L. Remmele, Jr., S. D. Bhat, D. H. Phan, W. R. Gombotz. Biochemistry 38 (1999) 5241

[25] R. L. Remmele, Jr., W. J. Callahan, S. Krishnan, L. Zhou, P. V. Bondarenko, A. C. Nichols, G. R. Kleemann, G. D. Pipes, S. Park, S. Fodor, E. Kras, D. N. Brems. J. Pharm. Sci. 95 (2006) 126.

[26] N. V. Buren, D. Rehder, H. Gadgil, M. Matsumura, J. Jacob. J. Pharm. Sci. 98 (2009) 3013.

[27] H. Hughes, C. Morgan, E. Brunyak, K. Barranco, E. Cohen, T. Edmunds, K. Lee. AAPS J. 11(2009) 335.

3 Separation and quantification of monoclonal-antibody aggregates by hollow-fiber-flow field-flow fractionation (Chapter 2)

3.1 Introduction

Study of therapeutic protein products, especially monoclonal antibodies, has recently attracted a great deal of attention from pharmaceutical industries. In the last 20 years, over 20 monoclonal antibodies have been approved in various therapeutic categories [1], and six antibody pharmaceuticals including Humira (adalimumab) and Remicade (infliximab) that make the top two of the sales of pharmaceuticals in 2012 [2]. These biopharmaceutical products have been drastically improving the quality of life of patients.

Compared to small pharmaceutical molecules, therapeutic protein products are considerably large entities with inherent physicochemical complexity. Therefore, many physical and chemical factors may lead to protein degradation and consequently affect the quality of therapeutic protein products during manufacturing, storage, shipping and handling steps [3-5]. Chemical degradation of proteins involves fragmentation, oxidation (mostly occurring at methionine and tryptophan residues), deamidation (mostly occurring at asparagine residues) and disulfide scrambling. Physical degradation of proteins involves unfolding, dissociation, denaturation, adsorption, precipitation processes and aggregates [5].

Aggregates are one of the most hazardous protein impurities of therapeutics because of its high risks of immune response or immunogenicity [6-10]. Therefore, the rapid development of therapeutic protein products leads to the demand for robust analytical methods for quantifying protein aggregates such as analytical ultracentrifugation-sedimentation velocity (AUC) and asymmetric flow field flow fractionation (AF4) to assess the risks of aggregates [11-15]. The authorities demand pharmaceutical companies to strictly quantify and qualify the aggregates of therapeutic protein products [16]. Size-exclusion high performance liquid chromatography (SE-HPLC) is a well-known method to quantify the amount of aggregates with high throughput capacity and quantitative performance. Therefore, SE-HPLC is an indispensable method and is frequently used for quantification of protein aggregates. However, SE-HPLC has several issues to be solved such as limited analytical range (<100 nm), interaction of proteins with silica-based resin pores of

the column (which may lead to a decrease in the recovery ratio of soluble and insoluble aggregates), and exposure to mobile phase containing high concentrations of salts (which may lead to protein aggregates or dissociation due to hydrophobic interaction) [17-20].

Nowadays, AUC and AF4 are widely used for quantification of protein aggregates as the orthogonal methods to SE-HPLC. In AUC experiments, a centrifugal force is used to accelerate sedimentation of very small particles such as protein molecules. Each protein species forms a unique boundary and sediment at a specific speed. The velocity of the moving boundary is characterized by the sedimentation coefficient governed by the molecular mass and shape [14]. An AUC assay can usually be performed without a matrix in most of formulation buffers with a minimal manipulation. Furthermore, a $c(s)$ distribution analysis on a recent analytical software (SEDFIT [21]) has provided improved resolution and can be applied to a wide variety of samples in distribution, because it can correct the broadening due to diffusion, and all the scans can be served for the analysis [11, 12]. Therefore, AUC with the $c(s)$ distribution analysis has been widely used in biopharmaceutical industries for the measurement of the size distribution of aggregates. However, AUC has still several issues to be solved in throughput and precision of analysis. The maximum number of samples for an assay is limited (seven). Technical skills for cell assembly and knowledge for the data analysis are required. In addition, the low precision of AUC requires large number of repeated analyses to get analytical data with acceptable precision. On the other hand, AF4 is a technique that can separate protein molecules based on their diffusion coefficients. The AF4 method does not use a stationary phase and thus has a broad dynamic range compared with SE-HPLC [15, 22]. AF4 is a high throughput method with high precision compared with AUC. However, proteins may interact with the membrane because the pressure (which presses protein molecules on the membrane) is generated by the flow field in AF4 experiments. In addition, professional skills are required to develop the AF4 method due to the complexity of the flow field and the affluence of setting parameters. The fact that the large quantity of the mobile phase is required for an assay is also one of the disadvantages in AF4.

Hollow fiber flow field flow fractionation (HF5) can also serve to separate protein molecules based on the diffusion coefficient. The principle and device of HF5 were constructed and developed

by Jan Åake Jönsson and Alf Carlshaf [23-26]. Although the principle of HF5 is similar to that of AF4, the membrane of HF5 is set cylindrically and the force of the HF5 cross flow is applied radially (in contrast, the force of the AF4 cross flow is applied vertically). The amount of the mobile phase per one test with HF5 is about one-third or one-fourth of that with AF4 and almost the same as that with SE-HPLC. In addition, one another advantage of HF5 is that the channel can be easily replaced with a new. Despite of these merits, HF5 seems to remain a minor method and only a few papers deal with the quantification of protein aggregates with HF5 [27]. The reason might be that HF5 instrumentation became commercially available only in the very last years and that the information on the separation conditions is limited.

In this study, we examined the effect of the setting parameters on fractographic characteristics and attempted to adjust the conditions of the HF5 method that can serve to separate antibody dimer and larger aggregates from monomer. We also precisely quantified the total amount of aggregates, and analyzed heat-induced antibody aggregate-containing samples with HF5 and compared the results with those of SE-HPLC, AUC and AF4.

3.2 Experimental

3.2.1 Chemicals and reagents

The pure standard sample of recombinant human monoclonal antibody (IgG1, Mab A) was obtained from Kyowa Hakko Kirin (Tokyo, Japan). Mab A was expressed in Chinese Hamster Ovary cells, cultured and purified by using a series of chromatographic and filtration steps. Mab A solution contained 10 mM sodium glutamate, 262 mM D-sorbitol, and 0.05 mg/mL polysorbate 80. Glutamate was selected from the buffer compounds commonly used in clinical antibody formulation. D-Sorbitol was selected from the tonicity agents commonly used in antibody formulation. Polysorbate 80 was added to prevent protein particle formation. All excipients conform to the United States Pharmacopeia 37 and National Formulary 32. Two Heat-induced Mab A aggregate-containing samples were prepared by heating Mab A for two weeks and one month at 60 °C, respectively. Other chemical reagents were of analytical reagent grade.

3.2.2 HF5

HF5 was performed on a Wyatt Technology Eclipse DUALTEC and an Agilent 1200 chromatography system. The chromatographic control, data acquisition and data analysis were performed using Chemstation (Agilent Technologies). For the separation, a hollow fiber cartridge (130 × 0.8 mm) used held a polyethersulfone membrane with a cutoff molecular mass of 10 kDa. The samples were set on an auto-sampler (as an accessory of the Agilent 1200 chromatography system), of which the temperature was set at 4 °C. The UV detector was operated at a wavelength of 215 nm. Phosphate buffer saline (PBS) was used as a mobile phase unless otherwise noted. The mobile phase was filtered with a 0.45-μm Millipore filter and degassed by an online degasser. The main flow rate, the cross flow rate, the focus flow rate, the focus point, and the injection amount were set at 0.7 mL/min, 0.5 mL/min, 1.2 mL/min, 15% and 2 μg, respectively, unless otherwise noted.

3.2.3 AUC

AUC was performed on a Beckman Coulter XL-A ultracentrifuge using 12-mm Epon charcoal-filled double-sector centerpieces with absorbance detection at 280 nm. The sample concentration was set at 0.5 mg/mL. The rotor speed and the rotor temperature were set for 40000 rpm and at 20 °C, respectively. The data analysis was carried out using a continuous $c(s)$ distribution model with the software program SEDFIT [21].

3.2.4 AF4

AF4 was performed with the Wyatt Technology Eclipse DUALTEC and the Agilent 1200 chromatography system. For the separation, a long channel equipped with a 350-μm spacer and a regenerated cellulose membrane with a cutoff molecular mass of 10 kDa was used. The mobile phase for the AF4 method was the PBS. Main flow rate, cross flow rate and focus flow rate were set at 1.2, 2.8, 2.8 mL/min, respectively. Focus point was set at 18% and injection amount of samples was set at 5 μg. The method run time was set to 60 min. Other conditions were set as the HF5.

3.3 Results and discussion

3.3.1 Optimization of setting parameters of HF5

The schematic diagrams of the HF5 procedure are given in Fig. S1. In HF5, the solvent is pumped through a channel allowing a part of the flow to penetrate the membrane. This creates a cross flow which is perpendicular to the main solvent flow that has a parabolic profile and is directed to the channel outlet. The combination of the two forces applied eventually results in the separation of the sample compounds based on the difference in the diffusion coefficient. At first, we analyzed a non-heated Mab A (pure standard sample) on HF5 under the conditions recommended for BSA in the manufacturer instruction. The recommended conditions are listed in Table 1. A fractogram under the recommended conditions for BSA is given in Fig. 1A. The shape of the monomer peak was broadened and collapsed.

Therefore, we examined the effect of the setting parameters including the main flow rate, the cross flow rate, the focus flow rate, the focus point, and the injection amount on the fractographic characteristics. As shown in Fig. 2A, with an increase in the main flow rate, the retention time decreased and the peak broadening occurred. An increase in the cross flow rate drastically caused the increase in the retention time and the resolution, as judged from Fig. 2B. These results show that the main flow rate and the cross flow rate are the key factors in the HF5 method, as reported by Dukjin Kang and Myeong Hee Moon [28]. Although the focus flow rate slightly affected the fractographic characteristics (Fig. 2C), we considered that the focus flow rate should be set to a value larger than the main flow rate to effectively focus protein samples, because sample would pass over the focus point before focusing at increased main flow rate compared with the focus flow rate. As shown in Fig. 2D, the effect of the focus point was not so remarkable, but at 15% of the focus point, the main peak height was larger and the peak resolution between the monomer and dimer peaks was better compared with those at 20% and 25%. Further shortening of the focus point caused an increase in the diffusion effect. Therefore, the focus point was set to 15%. As shown in Fig. 2E, the injection amount was also a significant factor in the separation. Although signal-to-noise ratio is in proportion to the injection amount, a better separation was achieved at 2-μg

injection between the monomer and dimer peaks in view of the signal-to-noise ratio and the resolution. In case of protein aggregate evaluation with AF4, the injection amount is usually set over 5 μg. However, the shape of the main peak at 5-μg injection with HF5 was collapsed. The difference seems to be due to the difference in the flow field form (cylindrical or rectangular), the diffusion direction with protein, and the speed of the several flows. All these factors affect the density of proteins during the focusing. At any rate, the injection amount should be optimized strictly.

The knowledge and information mentioned above are very useful for us to optimize the analytical conditions of HF5. During this work, we also realized that several subtle factors affected the separation characteristics in the HF5 method. The system pressure was tuned for each connected detector (diode array detector, florescence detector, or multi angle laser light scattering detector), and the direction of the hollow fiber cartridge affected the cross flow line (data not shown). We confirmed that the system pressure before the starting sequence should be within 16.5 to 17.5 bar (main flow rate: 0.7 mL/min, cross flow rate: 0.5 mL/min) and the cross flow line faced downward in all the experiments. These factors should be controlled strictly to improve reproducibility on HF5. In addition, the cartridge was conditioned by analyzing antibody aggregate-containing samples before acquiring all results in this work. These factors are also important to improve the reproducibility on HF5.

We optimized the HF5 conditions based on the knowledge on the characteristics of the setting parameters mentioned above. Table 1 summarizes the optimized conditions and Fig. 1B shows a fractogram of non-heated Mab A analyzed under the optimized conditions. The monomer peak became sharp, and a good separation was achieved between the dimer and the monomer peaks. The aggregation ratio of several commercial antibodies such as Synagis injection and Ritxan can also be evaluated under these optimized conditions.

Table 1 Analytical conditions of HF5 for antibodies

Analytical Conditions									
Conditions for BSA analysis at routine inspection					Optimized Conditions				
Time	Main Flow	Cross Flow	Focus Flow	Flow Type	Time	Main Flow	Cross Flow	Focus Flow	Flow Type
0.00	0.35	0.65	0.00	Elution	0.00	0.70	0.50	0.00	Elution
1.00	0.35	0.65	0.00	Elution	1.00	0.70	0.50	0.00	Elution
1.00	0.35	0.00	0.65	Focusing	1.01	0.70	0.00	1.20	Focusing
2.00	0.35	0.00	0.65	Focusing	2.00	0.70	0.00	1.20	Focusing
2.00	0.35	0.00	0.65	Focusing+Injection	2.00	0.70	0.00	1.20	Focusing+Injection
4.00	0.35	0.00	0.65	Focusing+Injection	4.00	0.70	0.00	1.20	Focusing+Injection
4.00	0.35	0.65	0.00	Elution	4.01	0.70	0.50	0.00	Elution
19.00	0.35	0.65	0.00	Elution	44.00	0.70	0.50	0.00	Elution
19.01	0.35	0.00	0.00	Elution+Injection	44.01	0.70	0.00	0.00	Elution+Injection
24.00	0.35	0.00	0.00	Elution+Injection	49.00	0.70	0.00	0.00	Elution+Injection
24.00	0.35	0.00	0.00	Elution	49.01	0.70	0.50	0.00	Elution
29.00	0.35	0.65	0.00	Elution	60.00	0.70	0.50	0.00	Elution

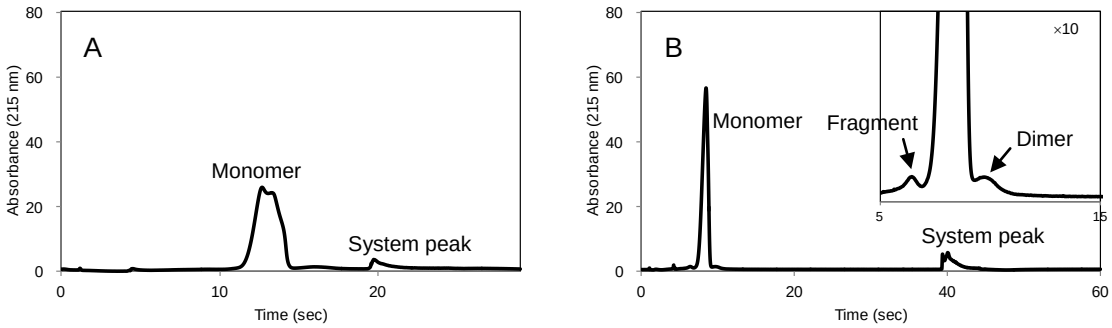

Fig. 1. Comparison of the fractograms of non-heated Mab A obtained under (A) the recommended conditions for BSA analysis at routine inspection and (B) the conditions optimized in this work. The details of the analytical conditions are summarized in Table 1.

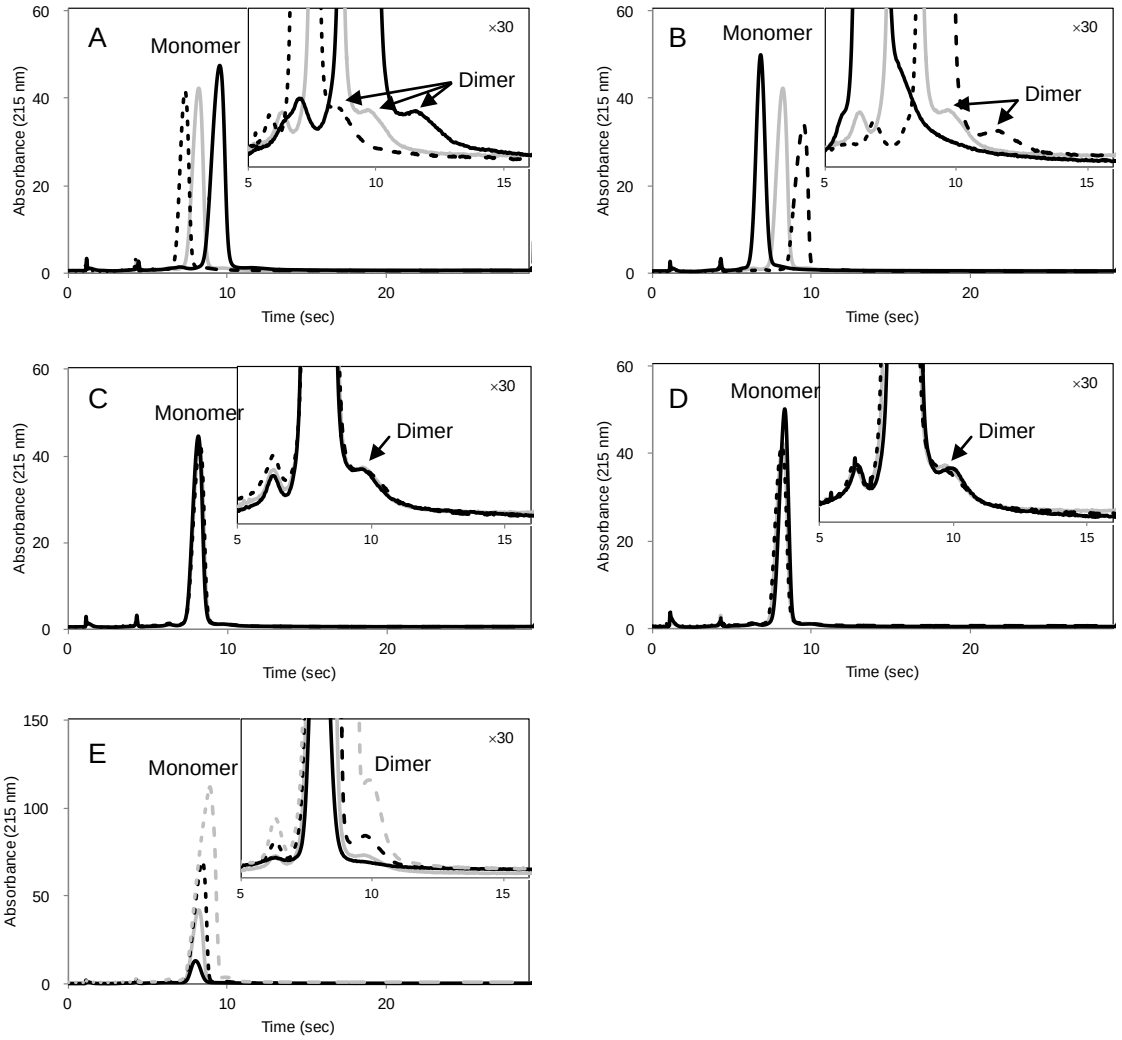

Fig 2. Effects of several setting parameters on the fractograms of non-heated Mab A with the HF5 method. Panel A: main flow rate dependence. The main flow rate is: (black solid line) 0.5 mL/min, (gray solid line) 0.7 mL/min, and (black dot line) 0.9 mL/min. Panel B: cross flow rate dependence. The cross flow rate is: (black solid line) 0.3 mL/min, (gray solid line) 0.5 mL/min, and (black dot line) 0.7 mL/min. Panel C: focus flow rate dependence. The focus flow rate is: (black solid line) 1.0 mL/min, (gray solid line) 1.2 mL/min, and (black dot line) 1.4 mL/min. Panel D: focus point dependence. The focus point is: (black solid line) 15%, (gray solid line) 20%, and (black dot line) 25%. Panel E: injection amount dependence. The injection amount is: (black solid line) 0.2 μg, (gray solid line) 1 μg, (black dot line) 2 μg, and (gray dot line) 5 μg. The standard conditions are: main flow rate = 0.7 mL/min, cross flow rate = 0.5 mL/min, focus flow =1.2 mL/min, focus point = 15%, and injection amount = 2 μg.

3.3.2 Verification of mobile phase condition of HF5 method

Åake Jönsson and Alf Carlshaf have already concluded the effects of the ionic strength of the mobile phase from the theoretical viewpoints [25]. However, they studied the effects not for protein samples but for polymer latex particles. Therefore, we examined the effect of the ionic strength and pH of the mobile phase on protein sample separation in the HF5 method. Fig. 3A and 3B revealed that pH is not an important factor, but the ionic strength extremely affected the peak shape, the recovery of the total area, the retention time, and the separation between the dimer and monomer peaks. With the mobile phase without NaCl, the peak height and the recovery of the total area were extremely low. Since Mab A (p*I*: 9.09 calculated from the amino acid sequence referred by [29]) has a positive charge in the mobile phase used, strongly attractive electrostatic interaction occurs with the negatively charged fiber wall membrane, especially at low ionic strength. This is the opposite situation in the polystyrene latex particles [25]. With the mobile phase containing 40 mM NaCl, the height of the monomer peak and the recovery of the total area increased most probably because NaCl could reduce the electrostatic interaction between Mab A and the membrane. However, the resolution between the dimer and monomer peaks became poor. With the mobile phase containing 140 mM NaCl, the dimer peak was separated well from the monomer peak. At increased concentration of NaCl (250 mM and 500 mM), the separation between the monomer and dimer peaks was poor. It is considered that the van der Waal's interaction between Mab A and Mab A increases under such high ionic strength conditions, and that the interaction may reduce the hydrodynamic volume of Mab A dimer compared with Mab A monomer, because the structural flexibility of the dimer is larger than that of the monomer. With a decrease in the difference of the hydrodynamic size between the dimer and the monomer, the separation becomes worse. These results indicate that the setting of the salt concentration in the mobile phase is also a key factor in the HF5 method, and that PBS (10 mM phosphate buffer, 140 mM NaCl, pH7.4) as the optimized mobile phase is the best compositions for the quantification of antibody aggregates.

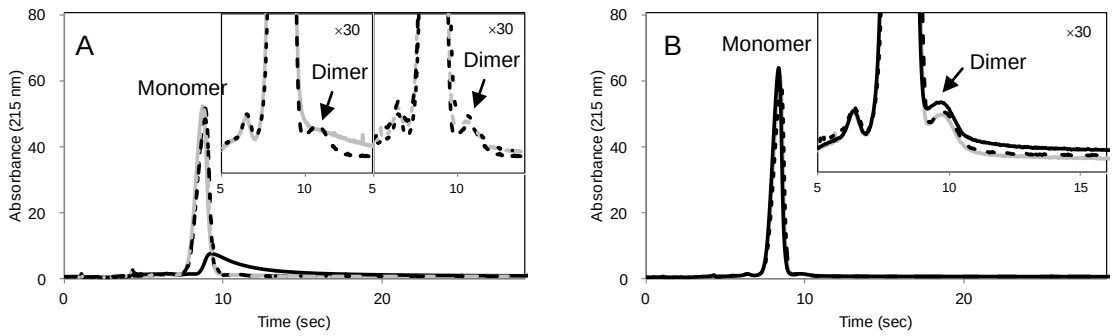

Fig 3. Effects of the NaCl concentration and pH of the mobile phase on the fractograms of non-heated Mab A with the HF5 method. Panel A: NaCl concentration dependence. The NaCl concentration is: (black solid line) 0 mM, (gray solid line) 40 mM, (black dot line) 140 mM, (gray dot line) 250 mM, and (black dash line) 500 mM. Panel B: pH dependence. The value of pH is: (black solid line) 6, (gray solid line) 7, and (black dot line) 8. The standard conditions are: NaCl = 140 mM, pH = 7. Other conditions are same as those in Fig. 2.

3.3.3 Qualification of HF5 method

Performance characteristics such as specificity, precision-repeatability, precision-intermediate precision, accuracy, linearity and quantitation limits of the HF5 method under optimized conditions were assessed to ensure that the method fits into its intended purpose to evaluate the aggregation ratio of the monoclonal antibody. Table 2 summarizes the method qualification results. The improved HF5 method provides satisfactory performance and it can be used to evaluate the aggregation ratio of monoclonal antibody samples.

Table 2 Summary of qualification results for the improved HF5 method

Performance	characteristics Qualification results
Specificity	No significant detectable interference observed with matrix
Linearity	R^2 of main peak area vs. protein load = 0.9998, R^2 of aggregates area vs. protein load = 0.9991 No significant trend observed in residual plot
Precision-repeatability	RSD of % main peak = 0.1%, RSD of % aggregates peaks = 0.9%
Precision-intermediate precision	RSD of % main peak = 0.2%, RSD of % aggregates peaks = 2.6%
Accuracy	main peak Accuracy = -3.5%, aggregates peaks Accuracy = -2.3%
Quantitation limit	Quantitation limit = 0.16% of total area at 2 μg protein load RSD of % aggregates (0.16% total area) = 5.7%, recovery % = 98.3%

3.3.4 Comparison HF5 to SE-HPLC, AUC and AF4

We evaluated the aggregation ratio of the pure standard Mab A sample and heat-induced Mab A aggregate-containing samples with HF5, SE-HPLC using two types of mobile phase, AUC and AF4. Here the aggregation ratio is defined and evaluated as area% of peaks eluted later than the monomer in HF5, AUC and AF4, while area% of peaks eluted earlier than monomer in SE-HPLC. The fractographic patterns are given in Fig. 4 and the detailed characteristics are summarized in Table 4. The aggregation ratios of the pure standard Mab A sample evaluated with the five methods were almost identical with each other. However, the standard deviation of AUC was higher than that of SE-HPLC, AF4 and HF5. For heat-induced Mab A aggregate-containing samples (60 °C 2 weeks and 60 °C 1 month), the aggregate ratios evaluated by SE-HPLC with moderate ionic strength-mobile phase (20 mM phosphate buffer, 300 mM NaCl) was evidently smaller than those evaluated by the other four methods. SE-HPLC may cause under-estimation of the aggregation ratio (especially for relative large aggregates eluted near void region) under irrelevant conditions. On the other hand, the aggregation ratios of non-heated Mab A and heat-induced Mab A aggregate-containing samples were suitably evaluated by HF5, AUC and AF4. The distribution extent of heat-induced Mab A aggregate-containing samples with HF5 was quite similar to those with AF4. AUC appears to show slightly better resolution than HF5, however, the reproducibility of the distribution extent with AUC was worse than that with HF5. These facts indicate that the HF5 method under the optimized conditions can be utilized in place of AUC and AF4.

Table 3 Summary of quantification results of the aggregation ratio with HF5, SE-HPLC, AUC, and AF4

	Aggregation peaks%		
Methods	Initial	60 °C, 2 weeks	60 °C, 1 month
HF5	1.7 ± 0.0	15.4 ± 0.4	31.5 ± 0.2
SE-HPLC1 (mobile phase : 20 mM Phosphate buffer, 300 mM NaCl)	1.6 ± 0.1	10.6 ± 0.2	19.8 ± 0.2
SE-HPLC2 (mobile phase : 50 mM Phosphate buffer, 500 mM NaCl)	1.7 ± 0.1	15.7 ± 0.4	32.3 ± 0.2
AUC	1.8 ± 1.7	15.2 ± 0.3	30.7 ± 2.5
AF4	1.7 ± 0.0	15.3 ± 0.4	32.5 ± 0.2

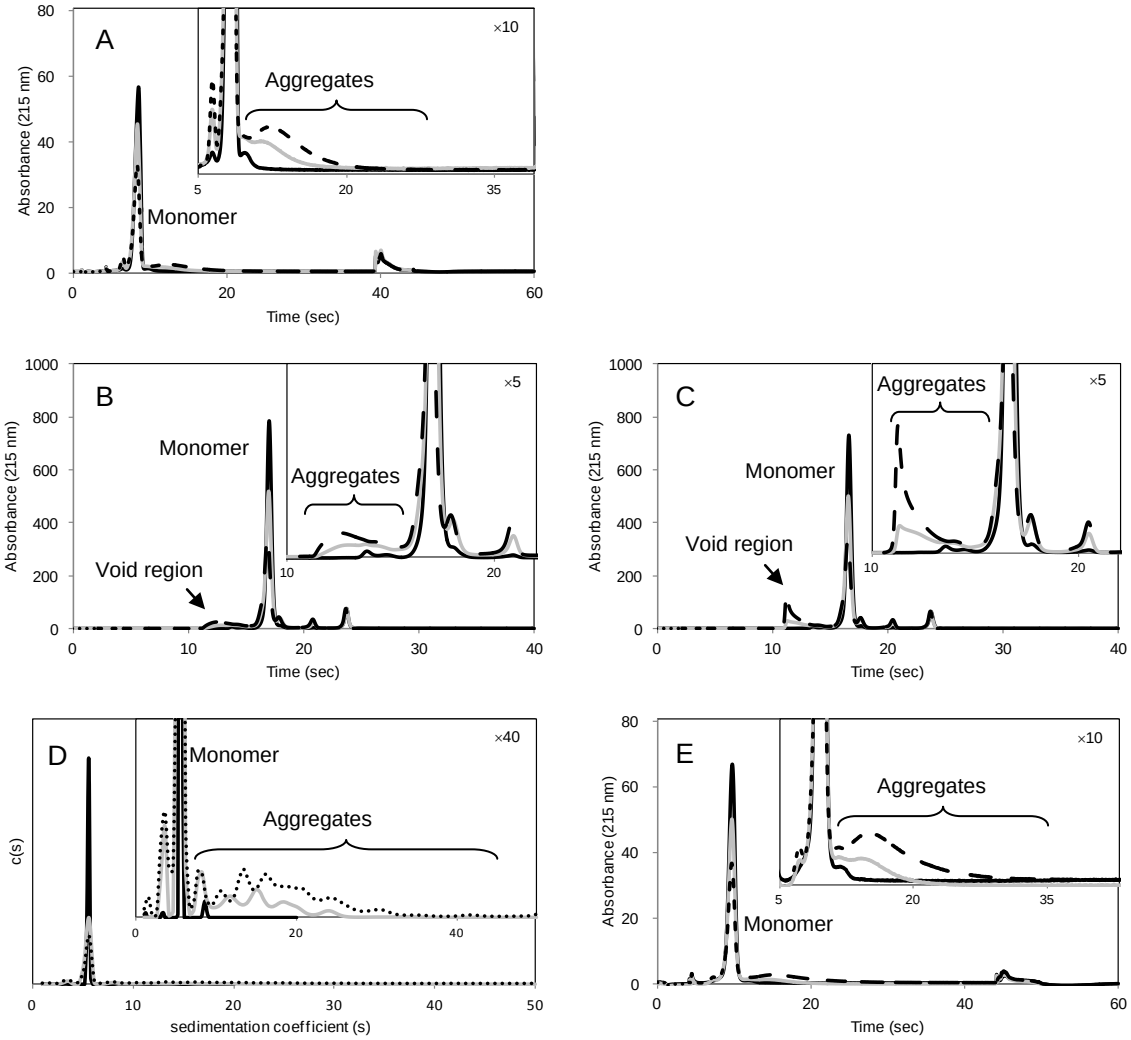

Fig. 4. Comparison with the fractograms of non-heated Mab A and heat-induced Mab A aggregate-containing samples (60 °C 2 weeks and 60 °C 1 month) recorded with five method/conditions. The separation methods are: (Panel A) HF5, (Panel B) SE-HPLC with a mobile phase containing 20 mM Phosphate buffer 300 mM NaCl, (Panel C) SEC-HPLC with a mobile phase containing 50 mM phosphate buffer 500 mM NaCl, (Panel D) AUC, and (Panel E) AF4. The analyte is: (black solid line) non-heated Mab A, (gray solid line) heat (60 °C, 2 weeks)-induced Mab A aggregate-containing sample, and (black dot line) heat (60 °C, 1 month)-induced Mab A aggregate-containing sample.

3.4 Reference

[1] Reichert JM (2008) Curr Pharm Biotechnol 9:423-430

[2] http://www.utobrain.co.jp/news/20130724.shtml

[3] Cromwell ME, Hilario E, Jacobson F (2006) AAPS J 8:E572–E579

[4] Wang W (1999) Int J Pharm 185:129–188

[5] Filipe V, Hawe A, Carpenter JF, Jiskoot W (2013) Tr Anal Chem 49:118–125

[6] Eon-Duval A, Broly H, Gleixner R (2012) Biotechnol Prog 28:608-622

[7] Rosenberg AS, Worobec A (2004) BioPharm Int 17:22-26

[8] Rosenberg AS (2006) AAPS J 8:E501-E507

[9] Carpenter JF, T. Randolph W, Jiskoot W, Crommelin DJA, Middaugh CR, Winter G, Fan YX, S Kirshner, Verthelyi D, Kozlowski S, Clouse KA, Swann PG, Rosenberg AS, Cherney B (2009) J PharmSci 98:1202-1205

[10] Singh SK, Afonina N, Awwad M, Bechtold-Peters K, Blue JT, Chou D, Cromwell M, Krause HJ, Mahler HC, Meyer BK, Narhi L, Nesta DP, Spitznagel T (2010) J PharmSci 99:3302-3321

[11] Schuck P (2000) Biophys J 78:1606-1619

[12] Lebowitz J, Lewis MS, Schuck P (2002) Protein Sci 11:2067-2079

[13] Liu J, Andya JD, Shire SJ (2006) AAPS J 8: E580-E589

[14] Arakawa T, Philo JS, Ejima D, Tsumoto K, Arisaka F (2007) BioProcess Int 5:36-47

[15] Arakawa T, Philo JS, Ejima D, Sato H, Tsumoto K (2007) BioProcess Int 4:52-70

[16] U S Department of Health and Human Services Food and Drug Administration, Center for Drug Evaluation and Research (CDER), Center for Biologics Evaluation and Research (CBER) (2013) “Guidance for Industry Immunogenicity Assessment for Therapeutic Protein Products”

[17] Arakawa T, Philo JS, Ejima, Tsumoto K, Arisaka F (2006) BioProcess Int 4:42-43

[18] Gabrielson JP, Brader ML, Pekar AH, Mathis KB, Winter G, Carpenter JF, Randolph TW (2007) J Pharm Sci 96:268-279

[19] Arakawa T, Ejima D, Li T, Philo JS (2009) J Pharm Sci 99:1674-1692

[20] Carpenter JF, Randolph TW, Jiskoot W, Crommelin DJ, Middaugh CR, Winter (2010) J Pharm Sci 99:2200-2208

[21] Schuck P http://www.analyticalultracentrifugation.com/default.htm

[22] Cao S, Pollastrini J, Jiang Y (2009) Curr Pharm Biotechnol 10:382-390

[23] Jönsson JÅ, Carlshaf A (1989) Anal Chem 61:11-18

[24] Carlshaf A, Jönsson JÅ (1989) J chromatogr A 461:89-93

[25] Carlshaf A, Jönsson JÅ (1991) J mirocolumn separations 3:411-416

[26] Carlshaf A, Jönsson JÅ (1993) Separation sci and technol 28:1031-1042

[27] Reschiglian P, Roda B, Zattoni A, Tanase M, Marassi V, Serani S (2014) Anal Bioanal Chem 406:1619-1627

[28] Kang D, Moon MH (2005) Anal Chem 77:4207-4212

[29] Henriksson G, Englund AK, Johansson G, Lundahl P (1995) Electrophoresis 16:1377-1380

4 Factors to govern soluble and insoluble aggregate-formation in monoclonal antibodies (Chapter 3)

4.1 Introduction

Study of therapeutic protein products, especially monoclonal antibodies (Mabs), has recently attracted a great deal of attention from pharmaceutical industries. In the last 20 years, over 20 Mabs have been approved in various therapeutic categories and hundreds of Mabs are currently in various stages of development [1]. Six antibody pharmaceuticals including Humira (adalimumab) and Remicade (infliximab) retain the top two market positions of pharmaceuticals in 2012 [2]. These biopharmaceutical products have been drastically improving the quality of life of patients.

Antibodies have been studied for over a century, and the basic structures and functions are now well understood [3-5]. Antibodies consist of two pairs of the light and heavy polypeptide chains which are held together through disulfide bridges. Light chains have two isotypes, λ and κ, which differ with each other in the sequence composition. Heavy chains are classified into five isotypes based on the chain structure and the effector function. All therapeutic Mabs currently approved belong to the immunoglobulin G (IgG) class. IgG has the simplest form among antibodies and is the major immunoglobulin type in human sera. IgGs are further divided into four subclasses, IgG1, IgG2, IgG3 and IgG4. The sequences of the light chain and the N-terminal domain of the heavy chains (called Fab domain) are variable, while the remaining domain are conserved. The variable domain, especially the complementarity determining region (CDR), determines the antigen binding specificity. Each IgG subclass has characteristic disulfide bonding pattern, which differs mostly in the hinge region [6,7].

Compared to small pharmaceutical molecules, therapeutic protein products such as Mabs are considerably large entities with inherent physicochemical complexity. Therefore, many physical and chemical characteristics may have significant relations to protein degradation and consequently affect the quality of therapeutic protein products during manufacturing, storage, shipping, and handling steps [8-10]. Chemical degradation of proteins involves fragmentation, oxidation (mostly occurring at methionine and tryptophan residues), deamidation (mostly occurring at asparagine

residues), and disulfide scrambling. Physical degradation of proteins involves unfolding, dissociation, denaturation, adsorption, precipitation processes, and aggregate formations [10].

Aggregates are one of the most hazardous protein impurities of therapeutics because of its high risks of immune response or immunogenicity [11-15]. It is important to prevent aggregation during the shelf-life of drug products. However, it takes a prolonged time for conducting long-term storage tests of biopharmaceutical products. Therefore, the stability test under accelerated conditions is generally applied to predict the long-term stability from the property of heat-stressed samples.

On the other hand, several methods are known to examine the degradation pathways by evaluating the characteristics of the biopharmaceutical products prior to the stability tests. The typical measures are the melting temperature (T_m) and the standard enthalpy of the melting point ($\Delta_m H°$) of the variable domains by differential scanning calorimetry (DSC). Since it has been considered that the increase in T_m results in the suppression of the agpIgregate formation and the denaturation, several trials including solvent selection are reported to increase T_m of each antibody domain, especially of the Fab domain [16,17]. Fluorescence spectroscopy with extrinsic fluorescent probe dyes such as 1-anilinonaphthalene-8-sulfonate (ANS), 4,4'-bis-1-anilinonaphthalene-8-sulfonate (bis-ANS), Nile Red, and Congo Red can also be employed as a highly sensitive method for protein characterization. Noncovalent hydrophobic or electrostatic interactions of the extrinsic dyes with proteins and protein degradation products are utilized for the characterization of pharmaceutical formulations [18]. Semisotnov et al. have revealed a strong affinity of ANS to the solvated hydrophobic core of molten globular intermediates of carbonic anhydrase B and α-lactalbumins [19]. The wavelength (λ_{max}) and the intensity (F_{int}) of the maximum florescence peak of the noncovalently bound extrinsic fluorescent dyes may be utilized as measures for protein characterization in screening tests in early stages of formulation development and in selection of formulation buffer suitable for biopharmaceutical products.

In formulation development, samples are dissolved in various kinds of solutions for DSC and fluorescence spectral test with dyes. However, the observed DSC and spectral parameters are affected not only by intrinsic conformational change of proteins but by solvent-related changes.

Therefore, DSC and fluorescence spectral tests should be performed with a given common solution. However, there are only few papers dealing with these parameters evaluated in a common solution for comprehensive assessment and prediction of Mabs aggregation [20, 21].

Recently, assessment and prediction of protein aggregation by computational approaches attract attention. For example, Wangv et al. have attempted to predict the susceptibility to the aggregation of commercial antibodies based on the information on the amino acid sequences and the Fab structures of potential aggregation-prone regions (APR) by using sequence-based computational tools [22]. This proposal is quite innovative because aggregation risk of each antibody can be predicted only from its amino acid sequence. However, in this study, we confirmed that some antibody with few aggregation prone regions easily aggregated under heat-stressed conditions. It thus appears to be risky to predict the tendency of the aggregation based on the information alone from the amino acid sequence of APR. Therefore, the combinational utilization of the sequence information and physical properties evaluated experimentally is important for more appropriate prediction of the aggregation propensity of proteins.

In this study, we used eight kinds of IgG1 antibodies as model protein pharmaceuticals, and five physicochemical parameters experimentally evaluated and two physicochemical parameters calculated based on the information from the amino acid sequence, as explanatory valuables to be related to the aggregate formation. The experimental parameters used are: T_m and $\Delta H°$ evaluated by DSC, λ_{max} and F_{int} evaluated by fluorescent spectroscopy with ANS; and the z-average diameter (D) evaluated by dynamic light scattering (DLS). All of the experimental parameters were obtained for the samples dissolved in a given phosphate buffer. The calculated parameters used are: the isoelectric point (pI) and the hydrophobicity of the CDR (H_{pho}) evaluated from the amino acid sequence of the antibody sample, since it has been reported that these parameters are strongly related with the formation of the protein aggregation [23-25]. The heat-stressed samples of the target antibodies were prepared and the soluble and insoluble aggregation formations were assessed by size exclusion chromatography (SE-HPLC). The aggregation formation data were correlated to the experimental and the calculated parameters. Multivariate analysis was done based on Akaike's Information Criterion (AIC) [26, 27] to pick out the important explanatory parameters to

characterize the aggregate formation. In this paper, we also discuss the mechanism and the potent approach to suppress the soluble and insoluble aggregate formation of IgG.

4.2 Experimental

4.2.1 Chemicals and reagents

The pure standard samples of six recombinant human Mabs (IgG1) were obtained from Kyowa Hakko Kirin (Tokyo, Japan). These antibodies were expressed in Chinese Hamster Ovary cells, cultured and purified by using a series of chromatographic and filtration steps. Synagis injection containing Palivizumab and Rituxan containing Rituximab were purchased from Abbvie (IL, USA) and F. Hoffmann-La Roche (Basel, Schweiz), respectively. All antibody samples were reconstituted with phosphate buffer saline (PBS; 10 mM Na_2HPO_4, 1.76 mM KH_2PO_4, 137 mM NaCl, 2.7 mM KCl, pH7.4; M = mol dm^{-3}) and named randomly as Mab A to H. Heat-induced Mab aggregate-containing samples were prepared by heat-induction of the native Mabs at 50 °C for typically one week, two weeks and one month. Other chemical reagents were of analytical reagent grade.

4.2.2 Size-exclusion chromatography

Size-exclusion chromatography (SE-HPLC) was performed with an Agilent 1100 chromatography system connected to a Tosoh TSKgel G3000SW_{XL} (300 × 7.8 mm, 5-μm particle size). The mobile phase was 50 mM NaH_2PO_4/Na_2HPO_4 (pH 7) containing 500 mM NaCl. The flow ratio was 1.0 mL/min and the column temperature was set at 25 °C. The injection amount of samples and the method run time were set at 20 μg and 20 min, respectively.

4.2.3 Differential scanning calorimetry

The thermal stability of individual domains was evaluated by differential scanning calorimetry (DSC). Measurements were performed on a 1.0 mg/mL IgG solution using a capillary VP-DSC system (MicroCal LLC, Northampton, MA) with a cell volume of 0.135 mL. The temperature scan was performed from 5 to 100 °C at a scan rate of 1 °C/min. A buffer–buffer reference scan was subtracted from the corresponding sample scan before the concentration normalization. Baselines

were created with Origin 7.0 (OriginLab, Northampton, MA) by cubic interpolation of the pre- and post-transition baselines.

4.2.4 Fluorescence probe spectrometry

Fluorescence measurements were performed on a Tecan Infinite 200 plate reader at an excitation wavelength of 380 nm. Emission intensity was collected in the range of 400–600 nm. The excitation bandwidth and the emission bandwidth were set as 9 nm and 20 nm, respectively. Measurements were performed at 25 °C. The samples were diluted by PBS containing ANS at 0.3 mg/mL (100 μM as the final concentration) and injected 100 μL each to the 96 well black plate /clear bottom.

4.2.5 Dynamic light scattering

Dynamic light scattering (DLS) analysis was performed on a DynaPro TM plate reader system equipped with an 832-nm laser using a 384-well bottom-read plate (Wyatt, Santa Barbara, CA). Measurements were performed at 25 °C. Each well contained 30 μL of a sample solution at a protein concentration of 10 mg/mL. The scattering data were fit (Dynamics software; Wyatt) assuming Rayleigh sphere scatterering.

4.3 Results and discussion

4.3.1 Physicochemical experimental characteristics of the antibodies

To characterize each antibody in terms of the conformational stability, the surface hydrophobicity, and the molecular size were measured by DSC, fluorescence assay with ANS, and DLS, respectively.

Figure 1 shows the DSC scanning patterns of the native antibody samples. The antibody sample solutions exhibited typical profiles with two or three transitions in the temperature range from 60 °C to 90 °C. The largest endothermic peak in each sample corresponds very likely to the thermal transition of the Fab domain as judged from the observed temperature and the magnitude of the peak, based on the literature [28-30]. Since the structural stability of the Fab domain makes a significant contribution to the structural stability of the antibody [20, 21, 29], we focused first on T_m

of the Fab domain as an index parameter of the structural stability of the antibody. The data are summarized in Table 1. T_m of the Fab domain of Mab B was 67.3 °C, which was the lowest among the eight antibodies. On the other hand, Mab E showed the highest T_m of the Fab domain (90.3 °C).

In addition, $\Delta_m H°$ representing the energy required for the structural change is another index parameter of the structural stability. It is generally considered that antibody with large $\Delta_m H°$ has the structural stability [29]. The evaluated $\Delta_m H°$ values are also summarized in Table 1. Mab B showed the lowest $\Delta_m H°$, while Mab E showed the highest value among the samples. The tendency is well correlated to that of T_m of the Fab domain.

Fluorescence spectra of ANS in the presence of the native antibody are given in Fig. 2. A significant blue shift and intensification of the fluorescence maximum peak are observed for Mab G, as compared with other antibodies. It is known that the blue shift of the ANS fluorescence is associated with its binding to a hydrophobic core of proteins [19]. Hence most likely, Mab G has significant hydrophobic regions on the protein surface compared with other Mabs. Mab B also shows a slight blue shift and intensification of the fluorescence maximum. On the other hand, no significant change was observed for other antibodies. The λ_{max} and F_{int} values are summarized in Table 1.

The DLS distribution patterns of the native antibody are given in Fig. 3. The *D* value was calculated from the particle size by using the Stokes-Einstein equation on the assumption that each molecule is in sphere. The any antibody used here has the same amino-acid sequence except the CDR with a similar molecular mass of about 150 kDa. However, as summarized in Table 1, it has been revealed that each antibody has a characteristic *D* value. Mab H gave a smallest *D* valuer, and Mab F gave the largest one.

Furthermore, the p*I* value of CDR was calculated from the amino acid sequence according to a method proposed by Henriksson G et al. [31]. The data are also summarized in Table 1. The CDR of Mab B gave a rather small value of p*I* (4.48) compared with the other antibodies. On the other hand, p*I* of CDR of Mab D, E, F, and G were located in a narrow region from 9 to 9.6. In addition, the hydrophobicity of the CDR was also calculated from the amino acid sequence according to the

method proposed by Kyte J et al. [32]. The data summarized in Table 1 show that the CDR of Mab B is most hydrophobic, and that of Mab H is most hydrophilic among the eight antibodies examined.

Table 1 Physicochemical parameters of each antibody

Method	Physicochemical parameters of each antibody						
	DSC		FL spectrum with ANS		DLS	Theretical values calculated by amino acid at CDR	
Patameter	T_m (°C)	$\Delta_m H°$ (kcal/mol)	F_λ (nm)	F_{int}	D (nm)	pI	H_{Pho}
Mab A	83.3	1.15	520	3488	12.0	6.49	-27.4
Mab B	67.3	1.01	510	5064	11.8	4.48	-18.2
Mab C	73.3	1.05	525	3473	12.3	7.56	-56.3
Mab D	78.8	1.13	520	3939	12.6	8.97	-56.5
Mab E	90.3	1.29	530	3334	12.2	8.97	-71.7
Mab F	79.1	1.04	520	3359	12.7	9.56	-20.0
Mab G	75.5	1.14	495	10803	12.3	9.18	-50.8
Mab H	83.3	1.12	520	3275	11.6	5.57	-23.2

F_λ: Maximum wavelength
F_{int}: Maximum intensity
D : z-average diameter
H_{pho}: Hydrophobicity

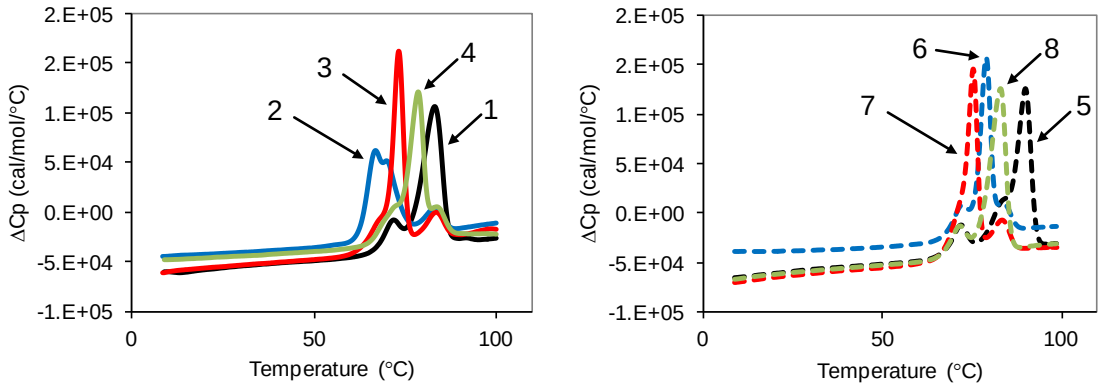

Fig. 1 DSC scans of each antibody (black solid line (1): Mab A, blue solid line (2): Mab B, red solid line: Mab C (3), green solid line (4): Mab D, black dash line (5): Mab E, blue dash line (6): Mab F, red dash line (7): Mab G, green dash line (8): Mab H)

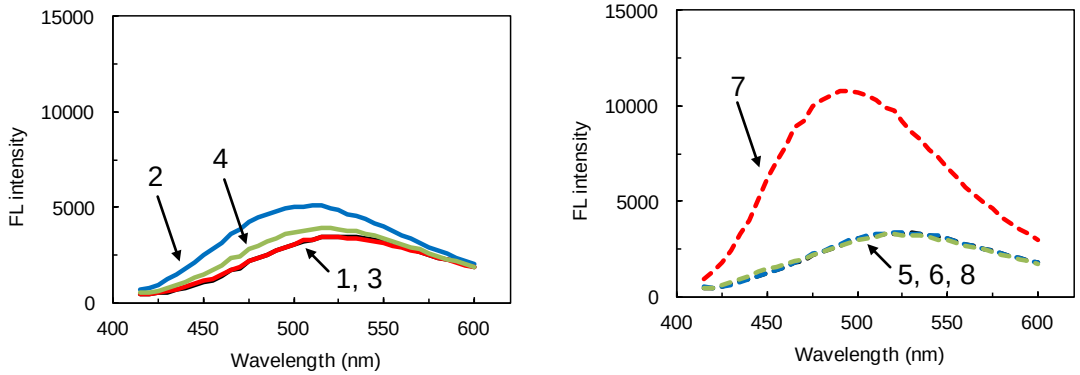

Fig. 2 Fluorescence spectra with ANS of each antibody (black solid line (1): Mab A, blue solid line (2): Mab B, red solid line: Mab C (3), green solid line (4): Mab D, black dash line (5): Mab E, blue dash line (6): Mab F, red dash line (7): Mab G, green dash line (8): Mab H)

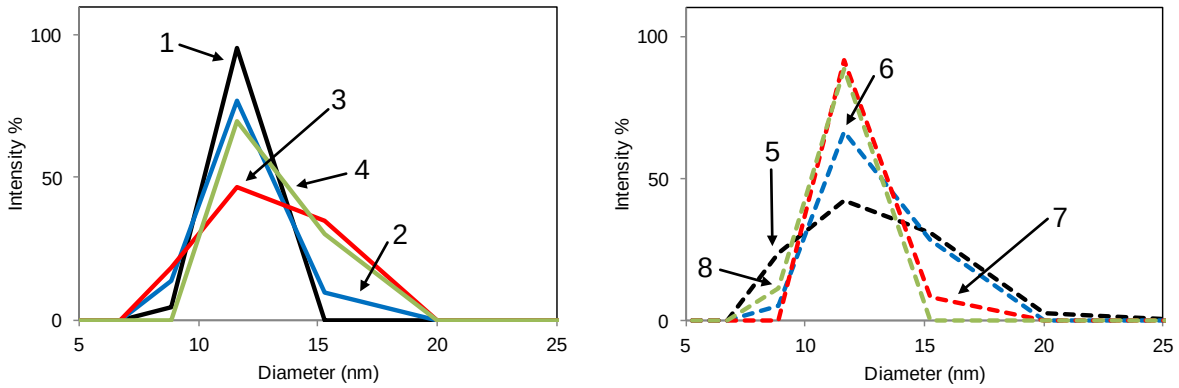

Fig. 3 Size intensity distributions by DLS of each antibody (black solid line (1): Mab A, blue solid line (2): Mab B, red solid line: Mab C (3), green solid line (4): Mab D, black dash line (5): Mab E, blue dash line (6): Mab F, red dash line (7): Mab G, green dash line (8): Mab H)

4.3.2 Soluble and insoluble aggregate formation in the heat–induced antibody samples

Figure 4 shows the SE-HPLC chromatograms of native and heat–induced aggregate-containing samples of Mab B and Mab G. In the case of Mab B (Panel A), the main peak of the monomer (at a retention time of about 7.8 min) decreased and the broad peaks (at retention times of 5-5.5 min) assigned to soluble aggregates increased with an increase in the heat-treatment time. The small peak at 6.7 min is assigned to dimer, and the peak area remain almost constant. By considering the time dependence of the peak area, the monomer is gradually denaturated in part during the heat treatment to form the multimeric and soluble aggregates via the dimeric aggregate. In the case of Mab G (panel B), the main peak of the monomer decreased with the heat-treatment time, but the broad peaks assigned to the soluble aggregates remained small. Therefore, the decrease in the main peak is mainly attributed to the formation of the insoluble aggregates, which could not be detected on the present SE-HPLC.

In this study, we will define a soluble aggregate ratio (A_s) by

$$A_s = P_n - P_s \qquad (1)$$

where P_s is the peak area of the broad soluble aggregates of the 1-month heat-treatment sample, and P_n is the peak area the native one. We also define an insoluble aggregate ratio (A_i) by

$$A_i = (P_n - P_h)/P_n \qquad (2)$$

where P_h is a total area of all peaks of heat-treatment samples. We also evaluated dA_s/dt and dA_i/dt as a kinetic index (rate constant) of the soluble and insoluble aggregate formation, respectively, where t is storage time of heat-treatment samples. Figure 5 shows dA_s/dt and dA_i/dt plots of Mab B and Mab G, and the data are summarized in Table 2. Mab B gave a significantly large value of dA_s/dt, indicating that Mab B is labile to form soluble aggregates during the heat treatment at 50 °C. On the other hand, Mab G gave a large dA_i/dt, indicating that Mab G is labile to form insoluble aggregates. Indeed, clear precipitates were observed in heat-induced aggregate-containing Mab G for 2 weeks and 1 month treatment at 50 ºC (data not shown).

Table 2 Physicochemical parameters of each antibody

Increment of soluble/insoluble aggregates (50 °C 0→1 month)		
Method	SE-HPLC	
Patameter	dA_s/dt (%/day)	dA_i/dt (%/day)
Mab A	0.288 ± 0.001	-0.196 ± 0.007
Mab B	1.146 ± 0.003	-0.382 ± 0.005
Mab C	0.583 ± 0.002	-0.176 ± 0.001
Mab D	0.320 ± 0.005	0.247 ± 0.007
Mab E	0.387 ± 0.001	-0.193 ± 0.011
Mab F	0.335 ± 0.001	-0.191 ± 0.012
Mab G	0.160 ± 0.013	0.858 ± 0.025
Mab H	0.346 ± 0.001	-0.143 ± 0.011

xxx ± xxx indicates average of slope value ± SD of slope value (n =3)

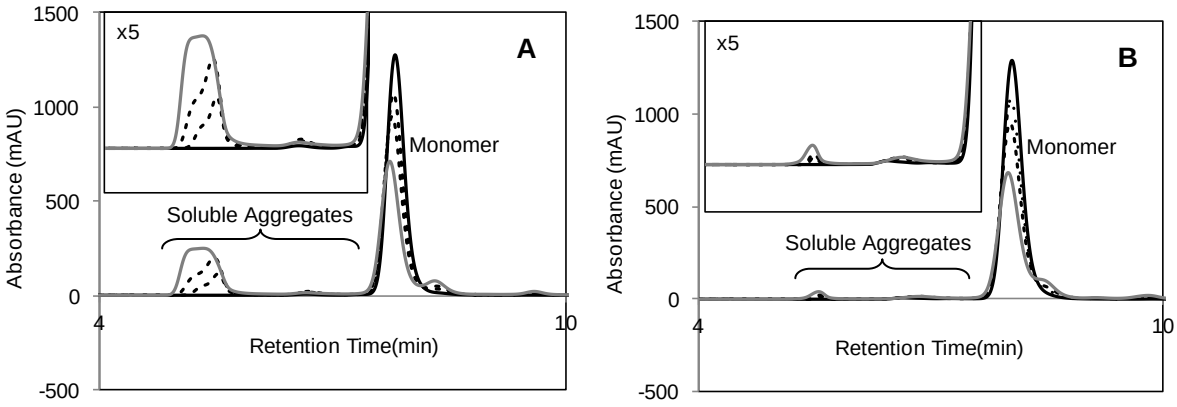

Fig. 4 The SE-HPLC chromatograms of non-heated and heat-induced aggregate-containing samples. Panel A shows Mab B, and panel B shows Mab G. The analyte is: (black solid line) non-heated, (black dash line) heat (50 °C, 1 week)-induced aggregate-containing sample, (black dot line) heat (50 °C, 2 weeks)-induced aggregate-containing sample and (grey solid line) heat (50 °C, 1 month)-induced aggregate-containing sample.

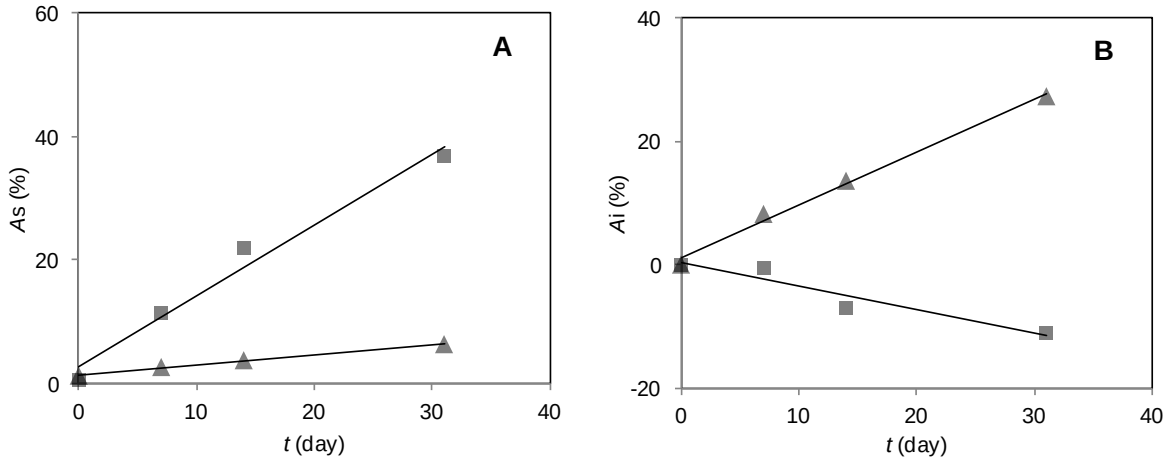

Fig. 5 The dA_s/dt (panel A) and dA_i/dt (panel B) plots of Mab B and Mab G. The analyte is: (gray squares) non-heated and heat (50 °C, 1 week, 2 weeks and 1 month)-induced aggregate-containing sample of Mab B, (gray triangles) non-heated and heat (50 °C, 1 week, 2 weeks and 1 month)-induced aggregate-containing sample of Mab G.

4.3.3 Statistical analysis and discussion

Table 3 summarizes correlation coefficients between the physicochemical parameters (T_m, $\Delta_m H°$, λ_{max}, F_{int} , D, pI, and H_{pho}) and between each of physicochemical parameters and each of the aggregation kinetic parameters (dA_s/dt and dA_i/dt). Strong correlations are recognized between T_m and $\Delta_m H°$ evaluated from DSC, and between λ_{max} and F_{int} evaluated by fluorescence probe spectroscopy. It seems to be reasonable to consider that an antibody with a high T_m is thermo-stable and then gives a large $\Delta_m H°$. It also seems to be reasonable to consider that interactions of ANS with hydrophobic binding sites within proteins accompanied by both an increase in fluorescence intensity and a blue shift of the peak maximum [18, 33].

Strong correlation is also observed between D and the calculated pI of CDR. The fact suggests that since all Mabs have molecular mass of about 150 kDa, the net charge of the CDR may affect the higher-order structure such as the angle of the hinge. The CDR is the antigen-recognizing site and thus locates on the surface of the antibody. The D value may change, when the angle of the hinge is changed by the electrostatic repulsive or attractive force between the CDR and the domains except for the CDR due to the charge of the CDR.

For the aggregation parameters, dA_i/dt is strongly related to F_{int}, but the correlations between dA_i/dt and each of other physicochemical parameters and between dA_s/dt and each of the physicochemical parameters are not so strong. Thus, we conducted multivariate analysis between the physicochemical characters as the explanatory variables and the aggregation parameters as the response variables by using Akaike's Information Criterion (AIC) [26, 27]. The parameters $\Delta_m H°$, λ_{max}, and D were excluded from the explanatory variables, because those are strongly correlated with T_m, F_{int}, and pI, respectively. Therefore, the physicochemical parameters used as the explanatory variables are: T_m, F_{int}, pI, and H_{pho} to correlate with the response variable dA_s/dt and dA_i/dt. Table 4 shows the result of multivariate analysis treated on R software (R i386 3.1.0) by using AIC. The AIC is defined by

$$\mathrm{AIC} = N \ln S + 2K \qquad (3)$$

where N, K, and S are the number of data, the number of explanatory variables, and the residual sum of the squares, respectively. When there are several competing models, the fitting model which gives the minimum AIC is a statistically maximum likelihood one. The AIC values for dA_s/dt were: –21.4 for K = 4 (T_m, F_{int}, pI, and H_{pho}), –22.2 for K = 3 (T_m, F_{int}, and pI), –22.2 for K = 2 (T_m and pI), and –20.8 for K =1 (pI). Therefore, the best expression is:

$$dA_s/dt = -0.0819\ \mathrm{p}I - 0.0203\ T_m + 2.67 \quad (R = 0.801) \qquad (4)$$

This regression equation means that antibodies with low pI and T_m are labile to form soluble aggregates. Since an antibody with low pI has positively charged CDR at neutral pH, the electrostatic interaction between the positively charged CDR and other negatively charged region may lead to the formation of soluble aggregates. Furthermore, the calculated pI values of whole antibody (Mab A to H) are from 9.0 to 9.4, so there are many negatively charged regions in the antibodies at neutral pH. Therefore, an increase in pH and the salt concentration of the solution might effective to -suppress the soluble aggregate formation. On the other hand, since T_m represents the thermo-stability of Fab, an antibody with high T_m may have resistance to the thermal denaturation, which leads to the soluble aggregate formation. It seems to be helpful for an antibody

with low T_m to be stored at low temperature. It would also be effective to find a solution composition to increase T_m of the target antibody.

The AIC values for dA_i/dt were: –21.3 for K = 4 (T_m, F_{int}, pI, and H_{pho}), –23.1 for K = 3 (T_m, F_{int} and pI), –24.6 for K = 2 (F_{int} and pI), and –21.9 for K =1 (F_{int}). Therefore, the best expression is:

$$dA_i/dt = 0.000119\ F_{int} + 0.0757\ pI - 1.14\ (R = 0.917) \quad (5)$$

This regression equation means that antibodies with large F_{int} and high pI are labile to form insoluble aggregates. The situation may lead to insoluble aggregate formation. Large F_{int} value means that the protein has rather large hydrophobic region (or core). Since an antibody with high pI of CDR has negatively charged CDR and other regions at neutral pH, repulsive force should be generated between each antibody molecule. However, in case that there exist some positively charged metal ions as ultra-trace impurities in solutions, the positively charged metal ions may mediate the formation of insoluble aggregates. There are several reports of metal ion–mediated aggregate formation [34, 35], and these metal ions are hard to be completely eliminated from buffer solutions.

Figure 6 shows the dA_s/dt and dA_i/dt plots of experimental values acquired by SE-HPLC versus theoretical values calculated by formula 4 and 5. The dA_i/dt plots indicates that one plot located upper right (Mab G) may greatly affect statistical analysis and correlation coefficient of dA_i/dt plots. Therefore, some antibody that forms insoluble aggregates slightly may not fit formula 5. Nevertheless, the formula can help for us to detect some antibody which has high risk of insoluble aggregate formation.

The aggregate formation pathway is generally considered as: “native” $\rightleftharpoons$ “denatured” $\rightarrow$ soluble aggregates $\rightarrow$ “insoluble aggregate”. This means that a reversible structural change from the native to a denatured form(s) triggers the soluble aggregate formation, and the insoluble aggregation is mediated by soluble aggregate formation [23]. Since antibodies with “low” pI and T_m are labile to form soluble aggregates and antibodies with large F_{int} and “high” pI are labile to form insoluble aggregates, this study shows that the explanatory variables strongly correlated with dA_s/dt are different from those correlated with dA_i/dt. Therefore, the rate determining step of the soluble aggregate formation is different from that of the insoluble aggregate formation. However, a

possibility cannot also be ruled out that the pathway of the soluble aggregate formation is inherently different from that of the insoluble aggregate formation. In the soluble aggregate formation, an electrostatic interaction seems to be a predominant one as the driving force and the kinetic barrier is reflected by the thermo-stability as expressed by T_m (or $\Delta_m H°$). On the other hand, the critical parameter of the insoluble aggregate formation seems to be the formation of hydrophobic core, and when the hydrophobic core mediates the aggregate formation, the insoluble aggregates may be formed predominantly. These discussions indicate that an approach to prevent the soluble aggregate formation should be different from that to prevent the insoluble aggregate formation. The stabilization of native antibody may be the key factor to prevent soluble aggregates, and the minimization of the hydrophobic core formation may be the key factor to prevent insoluble aggregates. Since antibodies with low or large p*I* are labile to form soluble or insoluble aggregates, respectively, it may also be effective to set the appropriate salt concentration of the solution for suppression of the soluble and insoluble aggregate formation. In addition, to make the p*I* of the CDR close to the neutral pH with some charged amino acid substitution may effective to suppress soluble and insoluble aggregate formation. In addition, some report indicates that amino acid substitution would increase the binding affinity between antigen and antibody [36, 37].

Table 3 Correlation coefficients of each physicochemical parameters and increment of soluble/insoluble aggregates (Gray: >0.800)

Correlation coefficients of each parameter									
Physicochemical parameters of each antibody								Increment of soluble/insoluble aggregates	
Method	DSC		FL spectrum with ANS		DLS	Theretical values calculated by amino acid at CDR		SE-HPLC	
Patameter	T_m (°C)	$\Delta_m H°$ (kcal/mol)	F_λ (nm)	F_{int}	D (nm)	pI	H_{Pho}	dA_s/dt (%/day)	dA_i/dt (%/day)
T_m (°C)	–	–	–	–	–	–	–	–	–
$\Delta_m H°$ (kcal/mol)	0.854	–	–	–	–	–	–	–	–
F_λ (nm)	0.544	0.294	–	–	–	–	–	–	–
F_{int}	0.358	0.012	0.923	–	–	–	–	–	–
D (nm)	0.015	0.016	0.062	0.067	–	–	–	–	–
pI	0.355	0.373	0.037	0.211	0.875	–	–	–	–
H_{Pho}	0.346	0.649	0.231	0.131	0.413	0.582	–	–	–
dA_s/dt (%/day)	0.645	0.531	0.010	0.181	0.383	0.672	0.321	–	–
dA_i/dt (%/day)	0.064	0.199	0.703	0.847	0.363	0.523	0.375	0.606	–

Table 4 Statistical analysis using the Akaike information criterion (Gray: lowest AIC)

Statistical Analysis with AIC				
Output parameter	dA_s/dt		dA_i/dt	
Input parameters (K)	T_m, F_{int}, pI, H_{pho}		T_m, F_{int}, pI, H_{pho}	
Start AIC (K=4)	-21.4		-21.3	
K=3	-22.2	(- H_{pho})	-23.1	(- H_{pho})
K=2	-22.2	(- F_{int})	-24.6	(- T_m)
K=1	-20.8	(- T_m)	-21.9	(- pI)
Final AIC	-22.2	(- H_{pho} - F_{int})	-24.6	(- H_{pho} - T_m)
Formula	$[dA_s/dt]$ = -0.0203 × [T_m] -0.0819 × [pI] + 2.67		$[dA_i/dt]$ = 0.000119 × [F_{int}] + 0.0757 × [pI] - 1.14	

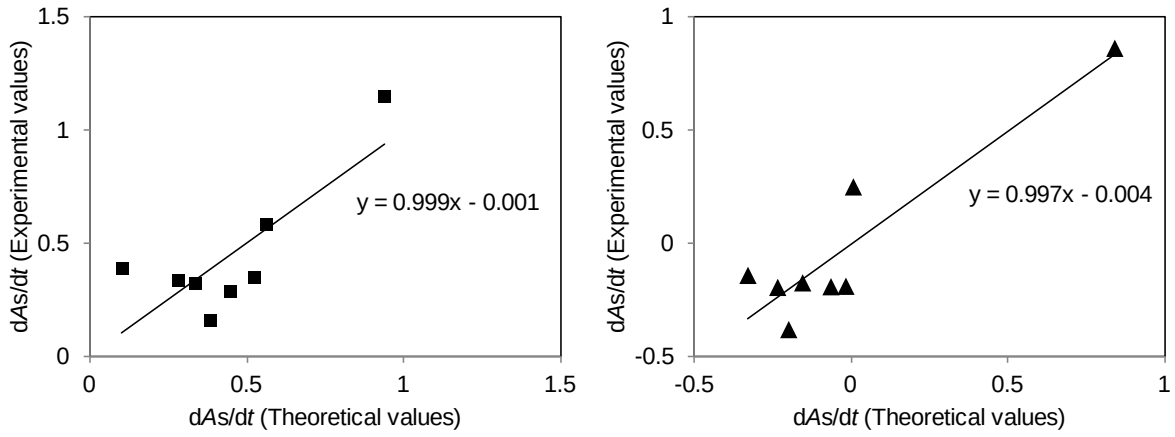

Fig. 6 The dA_s/dt (panel A) and dA_i/dt (panel B) plots of experimental values acquired by SE-HPLC (table 2) versus theoretical values calculated by formula 4 and 5. Black squares and triangles are Mab A ~ Mab H.

4.4 Reference

[1] Reichert JM. (2008) Curr Pharm Biotechnol, 9, 423-430.

[2] http://www.utobrain.co.jp/news/20130724.shtml

[3] Davies DR, Chacko S. (1993) Antibody structure. Acc Chem Res, 26, 421-7.

[4] Branden C, Tooze. (1998) J. Introduction to Protein Structure. Garland Publishing.

[5] Janeway CA, Travers P. Walport M, Sholmchik MJ. (2004) Immunobiology. Garland Science.

[6] Harris LJ, Larson SB, Hasel KW, Day J, Greenwood A, McPherson A. The threedimensional structure of an intact monoclonal antibody for canine lymphoma. Nature 1992; 360:369-72.

[7] Harris LJ, Skaletsky E, McPherson A. Crystallographic structure of an intact IgG1 monoclonal antibody. J Mol Biol 1998; 275:861-72.

[8] Cromwell ME, Hilario E, Jacobson F (2006) AAPS J 8:E572–E579

[9] Wang W (1999) Int J Pharm 185:129–188

[10] Filipe V, Hawe A, Carpenter JF, Jiskoot W (2013) Tr Anal Chem 49:118–125

[11] Eon-Duval A, Broly H, Gleixner R (2012) Biotechnol Prog 28:608-622

[12] Rosenberg AS, Worobec A (2004) BioPharm Int 17:22-26

[13] Rosenberg AS (2006) AAPS J 8:E501-E507

[14] Carpenter JF, T. Randolph W, Jiskoot W, Crommelin DJA, Middaugh CR, Winter G, Fan YX, S Kirshner, Verthelyi D, Kozlowski S, Clouse KA, Swann PG, Rosenberg AS, Cherney B (2009) J PharmSci 98:1202-1205

[15] Singh SK, Afonina N, Awwad M, Bechtold-Peters K, Blue JT, Chou D, Cromwell M, Krause HJ, Mahler HC, Meyer BK, Narhi L, Nesta DP, Spitznagel T (2010) J PharmSci 99:3302-3321

[16] He F, Woods CE, Trilisky E, Bower KM, Litowski JR, Kerwin BA, Becker GW, Narhi LO, Razinkov VI (2011) J PharmSci 100:1330-1340

[17] Ionescu RM, Vlasak J, Price C, Kirchmeier M (2008) J PharmSci 97:1414-1426

[18] Hawe A, Sutter M, Jiskoot W (2008) Pharmaceu. Res. 25:1487-1499

[19] Semisotnov GV, Rodionova NA, Kutyshenko VP, Ebert B, Blanck J, Ptitsyn OB (1990) FEBS Lett 224:9–13

[20] Ejima D, Tsumoto K, Fukada H, Yumioka R, Nagase K, Arakawa T, Philo JS (2007) Proteins: Structure, Function, and Bioinformatics 66:954-962

[21] Ito T, Tsumoto K (2013) Protein Sci. 22:1542-1551

[22] Wang X, Das TK, Singh SK, Kumar S (2009) mAbs 1:254-267

[23] Sahin E, Grillo AO, Perkins MD, Roberts CJ (2010) J. Pharm. Sci. 99, 4830–4848

[24] Caflisch A (2006) Curr. Opin. Chem. Biol. 10,437–444

[25] Roberts CJ (2014) Trends in Biotechnology Vol. 32, No. 7 372-380

[26] Akaike H (1974) IEEE Transactions on Automatic Control 19: 716–723.

[27] Hurvich CM, Tsai CL (1989) Biometrika 76; 297-307

[28] Vermeer AW, Norder W (2000) Biophys J 78:394–404.

[29] Garber E, Demarest JD (2007) Biochem Biophys Res Commun 355:751–757.

[30] Chennamsettya N, Voynova V, Kaysera V, Helkb B, Trouta BL (2009) PNAS 106; 11937–11942

[31] Henriksson G, Englund AK, Johansson G, Lundahl P (1995) Electrophoresis 16:1377-1380

[32] Kyte J, Doolittle F (1982) J. Mol. Biol. 157: 105-132

[33] Stryer L (1965) J. Mol. Biol 13:482–495

[34] Chi EY, Weickmann J, Carpenter JF, Manning MC, Randolph TW (2005) J PharmSci 94:256-274

[35] Tyagi AK, Randolph TW, Dong A, Maloney KM, Hitscherich C Jr., Carpenter JF (2009) J PharmSci 98:94-104

[36] Wells JA (1990) Biochemistry 29:8509–8517

[37] Carter PJ (2006) Nature Reviews Immunol. 6:343-357

5 Summary

5.1 Chapter 1

Size-exclusion chromatography (SE-HPLC) is a useful method for quantification of protein aggregates because of its high throughput capacity and highly quantitative performance. One of the problems in this method concerns polysorbates, which are well-known additives for protein-containing products to prevent protein aggregation, but frequently interfere with the photometric detection of protein aggregates. We developed a new SE-HPLC method that can separate polysorbates from protein sample solutions in an on-line mode with a precolumn with size exclusion and reversed-phase mixed modes. The precolumn can effectively trap polysorbates in aqueous mobile phase, and the trapped polysorbates are easily eluted with acetonitrile-containing aqueous mobile phase to clean the precolumn. Small parts of protein aggregates may be also trapped on the precolumn depending on temperature and proteins. Setting appropriate column temperature can minimizes such inconvenient trapping of aggregates.

5.2 Chapter 2

Hollow fiber flow field flow fractionation (HF5) serves to separate protein molecules on the basis of the difference in the diffusion coefficient and can evaluate the aggregation ratio of proteins. However, HF5 is still minor because the information on the separation conditions is limited. We examined in detail the effects of various setting parameters including the main flow rate, the cross flow rate, the focus point, the injection amount, and the ionic strength of the mobile phase on fractographic characteristics. Based on the results, we proposed the optimized conditions of the HF5 method for the quantification of monoclonal antibody in sample solutions. The HF5 method was qualified in view of the precision, the accuracy, the linearity of the main peak, and the quantitation limit. In addition, the HF5 method was applied to non-heated Mab A and heat-induced antibody aggregate-containing samples to evaluate the aggregation ratio and the distribution extent. The separation performance was comparable with or better than that of the conventional methods such as analytical ultracentrifugation-sedimentation velocity and asymmetric flow field flow fractionation.

5.3 Chapter 3

The aggregation formation of monoclonal antibodies as biopharmaceuticals induced by heat stress was evaluated by size-exclusion chromatography, and was correlated with several physicochemical parameters of the antibodies to clarify the factors to govern the aggregate formation. The parameters to which we paid attention are: the melting temperature (T_m) and the standard enthalpy of the melting point ($\Delta_m H°$) evaluated by differential scanning calorimetry under given and common conditions; the wavelength (λ_{max}) and the intensity (F_{int}) of the maximum florescence peak of 1-anilinonaphthalene-8-sulfonate as a probe dye; the z-average diameter (D) evaluated by dynamic light scattering; and the isoelectric point (pI) and the hydrophobic index (H_{pho}) of the complementarity determining region calculated from the amino acid sequence. Multivariate statistical analysis with these explanatory variables based on Akaike's information criterion indicates that the soluble aggregate formation is correlated with T_m and pI, while the insoluble aggregate formation is correlated with F_{int} and pI. Based on these results, mechanisms of and measures to prevent the aggregate formation are discussed.

6 Conclusion

6.1 Chapter 1

We have proposed an improvement of the conventional SE-HPLC method for analysis of protein aggregates in protein-based samples containing some detergents such as PS80 and PS20 by using MSpak GF-4A as a precolumn. The method performs an on-line analysis of protein aggregates. The mixed modes based on size exclusion phase and reversed-phase seem to effectively work to trap the detergents. However, some hydrophobic interaction between protein aggregates (especially with hydrophobic nature) and the stationary phase of the precolumn might cause to trap the protein aggregates in part. This work has also revealed that such interference can be minimized by tuning the column temperature.

6.2 Chapter 2

We have revealed the effects of several setting parameters of the HF5 method on the fractographic characteristics including the retention time, the peak shape, and the separation between the dimer and monomer peaks. Finally, we have proposed the optimized conditions of the HF5 method for analysis of antibody aggregates. This work and information are very useful for development of the HF5 method for wide range of protein aggregate evaluation. We have also qualified the proposed HF5 method and confirmed that the method provides satisfactory performance and that it can be used to evaluate the aggregation ratio of monoclonal antibodies. In addition, we have clarified that the antibody aggregates can be evaluated with HF5 method, and that HF5 method can replace SE-HPLC, AUC and AF4 to compare the aggregation ratio of non-heated and heat-induced antibody aggregate-containing samples.

6.3 Chapter 3

As for antibodies in the same class, an amino acid sequence of more than 90% is stored in theprimary structure, and that the difference in the amino acid composition is almost limited in the CDR. However, the difference causes the difference in the electrostatic and hydrophobic interactions, which leads to the large variety of the thermo-stability, the high-order structure, and the z-average diameter. It is reconfirmed that these differences contribute to the difference in the

soluble and insoluble aggregate formation. We have also confirmed that the soluble aggregate formation induced by heat stress is correlated to the thermo-stability of the Fab domain and p*I* of the CDR, and the insoluble aggregate formation is correlated with the hydrophobic core (high-order structure) of the antibody and the hydrophobicity of the CDR. These results suggest that the rate-determining step, or more strongly, the pathway of the soluble and the insoluble aggregate formation is different from each other, and that the prediction of the risk of the soluble and insoluble aggregate formation of antibody seems to be possible. Since the present approach to predict the aggregation formation has acceptable reliability and requires only a small amount of test sample in a short time, it would be very useful for selecting an appropriate cell to express a target antibody with high resistance to the aggregate formation from a large variety of candidates.

7 Acknowledgement

I started Ph. D. study in the spring of 2012. During the course of study, I have received hearty encouragements from many people. First of all, I would like to express my sincere gratitude to Professor Kenji Kano (Graduate School of Agriculture, Kyoto University) for his continuous instruction, discussion, encouragement and tough love through this study. He has continuously helped my scientific insight and my character build since I was twenty-two year old. He is like father to me. I owe my gratitude to Associate Professor Osamu Shirai (Graduate School of Agriculture, Kyoto University), Research Associate Yuki Kitazumi and Ms Toshie Koyama for their encouragement.

I am very much grateful to my collaborators, Dr. Shigehiro Yanagihara (Kyowa Hakko Kirin Co., Ltd.) and Dr. Takafumi Iwura (Kyowa Hakko Kirin Co., Ltd.), for their great supports, encouragements, helpful discussion and technical supports. I greatly respect them and I want to keep up with them.

I also give special thanks to Mr. Yukihito Ohyama (Kyowa Hakko Kirin Co., Ltd.), Dr. Noriko Ohtani (Kyowa Hakko Kirin Co., Ltd.), Dr. Katsuyoshi Yamazaki (Kyowa Hakko Kirin Co., Ltd.), Dr. Yuuki Yagi (Kyowa Hakko Kirin Co., Ltd.), Mr. Daisuke Tsutida (Kyowa Hakko Kirin Co., Ltd.), Mr. Hiroyuki Suetomo (Kyowa Hakko Kirin Co., Ltd.), Mr. Takayuki Muro (Kyowa Hakko Kirin Co., Ltd.) and Mr. Shunsuke Ozaki (Eisai Co., Ltd) for their great supports and encouragements.

I would like to thank members of Kano laboratory and Kyowa Hakko Kirin Co., Ltd analytical science group for their encouragements.

Finally, I thank my parents, Dr. Hiroo Fukuda, Ms. Ikuko Fukuda, and my wife, Ms. Mie Fukuda (Kyowa Hakko Kirin Co., Ltd.) for their great supports and warmhearted encouragements.

8 List of publications

8.1 Original publications

1 J. Fukuda, T. Iwura, S. Yanagihara, K. Kano

Utilization of a precolumn with size exclusion and reversed-phase modes for size-exclusion chromatographic analysis of polysorbate-containing protein aggregates

Journal of Chromatography B, **953–954**;68–72 (2014)

2 J. Fukuda, T. Iwura, S. Yanagihara, K. Kano

Separation and quantification of monoclonal-antibody aggregates by hollow-fiber-flow field-flow fractionation

Analytical and Bioanalytical Chemistry, **406**;6257–6264 (2014)

3 J. Fukuda, T. Iwura, S. Yanagihara, K. Kano

Prediction of soluble and insoluble aggregate-formation in antibody solutions with bioAnalytical techniques and statistical analysis

(in preparation)

8.2 Other publications

1 J. Fukuda, S. Tsujimura, K. Kano

Coulometric bioelectrocatalytic reactions based on NAD-dependent dehydrogenases in tricarboxylic acid cycle

Electrochimica Acta, **54**;328–333 (2008)

2 S. Tsujimura, J. Fukuda, O. Shirai, K. Kano

Micro-coulometric study of bioelectrochemical reaction coupled with TCA cycle

Biosensors and Bioelectronics, **34**;244–248 (2012)

3 T. Iwura, J. Fukuda, K. Yamazaki, S. Kanamaru, F. Arisaka

Intermolecular interactions and conformation of antibody dimers present in IgG1 biopharmaceuticals

The Jounal of Biochemistry, **155**;63–71 (2014)

4 T. Iwura, J. Fukuda, K. Yamazaki, F. Arisaka

Conformational stability, reversibility and heat-induced aggregation of α-1-acid glycoprotein

The Jounal of Biochemistry, **156**;345–352 (2014)